

Frugal, Flexible, Faithful: Causal Data Simulation via Fregression

Linying Yang^{*1}, Robin J. Evans^{*1,2}, and Xinwei Shen^{*3}

¹Department of Statistics, University of Oxford

²Pioneer Centre for SMARTbiomed, University of Oxford

³Department of Statistics, University of Washington

August 5, 2025

Abstract

Machine learning has revitalized causal inference by combining flexible models and principled estimators, yet robust benchmarking and evaluation remain challenging with real-world data. In this work, we introduce fregression, a deep generative realization of the frugal parameterization that models the joint distribution of covariates, treatments and outcomes around the causal margin of interest. Fregression provides accurate estimation and flexible, faithful simulation of multivariate, time-varying data; it also enables direct sampling from user-specified interventional distributions. Model consistency and extrapolation guarantees are established, with validation on real-world clinical trial data demonstrating fregression’s practical utility. We envision this framework sparking new research into generative approaches for causal margin modelling.

1 Introduction

The use of machine learning tools has given causal inference a new lease of life, enabling complex models to be used with principled causal estimators and guarantees about statistically important quantities (Wager and Athey, 2018; Chernozhukov et al., 2018; Hahn et al., 2020). To build trustworthy causal models, however, we also need to understand when these methods may be more or less reliable, or perhaps fail completely. This implies that causal inference needs a set of good benchmarking tools. Unfortunately, real-world datasets are not ideal for this task, because they cannot give us access to the ground truth other than in a few very special circumstances. In particular, they rarely provide the counterfactual outcomes we care about, and the distribution we want to evaluate often differs from the one that produced the observations. Well-designed simulations can address this discrepancy (Neal et al., 2020; Parikh et al., 2022); they allow us to choose a ground truth, stress-test new methods, compare their generalizability and stability, and expose failure modes before deployment. In trial design, simulations also guide sample size calculations, making patient recruitment more efficient. Valid benchmarks have therefore become

^{*}E-mails: linying.yang@stats.ox.ac.uk, evans@stats.ox.ac.uk, xwshen@uw.edu

central to method development in the AI era. Faithful simulation is no longer optional; it is a core step in building trustworthy causal models (Friedrich and Friede, 2024; Pezoulas et al., 2024; Gamella et al., 2025).

Generating data that obeys a marginal interventional distribution, rather than merely reproducing conditional relationships, is not an easy task (Havercroft and Didelez, 2012). Evans and Didelez (2024)'s *frugal parameterization* provides a solution to this challenge by centring on the causal margin and adjusting the surrounding variables accordingly. This framework allows us to sample data from the target distribution, incorporate time-varying covariates coherently, and ensures that subsequent inference targets the specified causal quantity (Lin et al., 2025). Consider covariates $Z \in \mathbb{R}^{d_z}$, treatment $X \in \mathbb{R}^{d_x}$, and outcome $Y \in \mathbb{R}^{d_y}$, along with their corresponding supports \mathcal{Z} , \mathcal{X} , \mathcal{Y} . The frugal parameterization decomposes the joint distribution \mathbb{P} of (Z, X, Y) into three components: 'the past' \mathbb{P}_{ZX} , which is the joint distribution of treatment and covariates that occur causally prior to the outcome Y ; the causal distribution of interest $\mathbb{P}_{Y|X}^*$; and a (conditional) dependency parameter denoted by $\phi_{ZY|X}^*$. In line with Evans and Didelez (2024), we mark quantities from the interventional (causal) distribution with an asterisk (*) and leave observational quantities unmarked. This parameterization allows data simulation with the marginal causal quantity specified. We note that, just as with the original frugal parameterization, the treatment can include some elements of the covariates, leading to a causal estimand that is conditional on those variables.

The ability to *simulate* realistic data and to *estimate* causal parameters accurately are two sides of the same coin. Only by fitting the observational distribution well via flexible, robust estimators can we generate high-fidelity simulations that reproduce confounding structures, time-varying effects, and real-world heterogeneity. Those simulations, in turn, furnish ground-truth scenarios for stress-testing methods. In the original frugal parameterization, all the models were parametric and low-dimensional. While elegant and interpretable, its reliance on predefined functional forms can limit flexibility when fitting on real-data. In this paper, we introduce *fregression*, a new approach for frugal parameterization using deep generative models. Building on the distributional regression foundations of engression (Shen and Meinshausen, 2024), fregression requires minimal tuning, extrapolates beyond the observed support, and delivers superior performance in both data simulation and causal estimation.

1.1 Contribution

Fregression combines directly targeting the estimation of marginal causal quantities of interest, with the capacity to generate complex benchmark datasets, and so that the marginal causal distributions can be user-specified. This unified framework guarantees a precisely defined marginal effect while closely reflecting real-world conditions. Consistent with the frugal parameterization, fregression consists of variation independent components to isolate and control specific causal properties, such as the strength of confounding.

We highlight some key properties of fregression:

- **Generative model for causal margin.** Fregression is a flexible deep generative model

for distributional regression that represents the entire outcome distribution while explicitly specifying the marginal interventional distribution of interest. Directly targeting the marginal quantity of interest allows for better estimation and more precise control.

- **Broad applicability.** Our framework supports both estimation and simulation for a variety of (complex) settings, including distributional treatment effects, continuous treatments, longitudinal settings, and survival data.
- **Flexibility and robustness.** Fregression factorizes the joint distribution according to a frugal, variation independent parameterization, enabling each component to be modelled with any suitable method (not limited to neural networks). The model fitting does not require extensive hyperparameter tuning, enhancing overall stability.
- **Theoretical guarantees.** We provide a consistency guarantee for models trained with the finite-sample energy score, along with extrapolation guarantees under continuous treatments.

1.2 Related Work

We review existing approaches to generative modelling for causal estimation and simulation and how they motivate our fregression framework. We summarize this comparison between fregression and other methods in Table 1.

Method	Binary Treatment	Continuous Treatment	Longitudinal Data	Distributional Treatment Effects	Extrapolation	Modelling Causal Margin
TARNet						
CFRNet						
Dragonnet	✓	✗	✗	✗	✗	✗
CEVAE						
CausalEGM	✓	✓	✗	✗	✗	✗
CausalBGM						
RealCause	✓	✗	✗	✗	✗	✗
Credence						
DeepACE	✓	✗	only static treatment regime	✗	✗	✗
Deep LTMLE	✓	✗	✓	✗	✗	✗
Frugal Flow	✓	✓	✗	✗	✗	✓
Fregression	✓	✓	✓	✓	✓	✓

Table 1: Comparison of methods.

1.2.1 (Deep) generative models for the causal margin

Deep learning models have shown remarkable flexibility for causal estimation in high-dimensional, complex settings. For instance, TARNet and CFRNet learn shared representations that balance treated and control groups (Shalit et al., 2017), and Dragonnet incorporates the propensity score estimation directly into the outcome network (Shi et al., 2019). However, since they enforce covariate balance across treatment arms to mitigate confounding, these architectures are limited to binary treatments and static covariates; in particular, they cannot handle longitudinal data.

Generative models offer a natural framework for modelling causal relationships. Indeed, structural equation models (Pearl, 2009) can be viewed in this way: the most straightforward method

is to build generative models directly for the structural equations of each variable. In the nonparametric instrumental variable (IV) setting, Holovchak et al. (2025) applied this idea by proposing a distributional IV method that estimates the full (conditional) interventional distribution in the presence of latent confounders. Other existing generative models for causal effect estimation include: CEVAE, which uses variational autoencoders to recover the joint distribution of observed and latent confounders from purely observational data (Louizos et al., 2017); CausalEGM (Liu et al., 2024) encodes confounders into a low dimensional latent space via an encoder–generator architecture, dropping any treatment specific network structure and thus accommodating continuous treatments (e.g. dosage levels). Its recent extension, CausalBGM (Liu and Wong, 2025), augments this approach with a Bayesian neural network in order to output both the both the mean and variance of individual treatment-effect posteriors, assuming their distributions to be Gaussian.

All these methods above focus on the *conditional* interventional distribution. By contrast, modelling the *marginal* interventional distribution via generative models is much less straightforward. When we marginalize out covariates, the causal margin is in general not directly induced from the structural equation of the outcome. Concretely, if $Y = f(X, Z, \varepsilon_Y)$, where ε_Y is the exogenous noise variable, sampling from $\mathbb{P}_{Y(x)|Z=z}$ is as simple as drawing ε_Y from its margin and computing $f(x, z, \varepsilon_Y)$. To sample from the marginal $\mathbb{P}_{Y(x)}$, however, we must simulate from the interventional distribution $Z(x)$. Thus, the generative mechanism that induces the causal margin dose not in general coincide with the original structural form. Fregression, instead, provides a novel way to address this by explicitly constructing a generative model for the causal margin with a reparameterized independent noise variable. In addition, the variation independence of each of our model components allows flexible specification of that margin while faithfully simulating causal data.

1.2.2 Modelling longitudinal data

Causal estimation in longitudinal settings remains relatively underdeveloped. Motivated by LTMLE (Longitudinal Targeted Maximum Likelihood Estimation, van der Laan and Gruber, 2012; Lendle et al., 2017) and iterative g-computation, Frauen et al. (2023) proposed DeepACE, leveraging recurrent neural networks to capture patient trajectories and estimate the average risk ratios. A limitation is that it can only deal with static treatment regimes. Shirakawa et al. (2024) introduced Deep LTMLE as extensions on LTMLE and DeepACE, using transformer architectures to estimate the counterfactual mean outcomes under dynamic treatment policies in longitudinal settings. However, these methods generally rely on empirically averaging potential outcomes conditioned on covariates for estimating the marginal causal quantities, demand sensitive hyperparameter tuning, and do not enable data simulation.

By contrast, fregression’s frugal parameterization naturally extends to longitudinal data: it supports a wide range of estimands—including marginal and conditional effects under both static and dynamic regimes—and permits straightforward data simulation, all without elaborate tuning.

1.2.3 Modelling distributional treatment effects

Most causal estimation methods focus on average treatment effects, but distributional treatment effects (DTE) have become increasingly important for richer insights beyond the mean (Abadie, 2002; Bitler et al., 2017). Recent works on analyzing DTE include semiparametric models (Díaz, 2017; Kennedy et al., 2023), which depend critically on correct model specification; kernel-based approaches dispense with parametric assumptions and can test for distributional shifts nonparametrically, but they often suffer from poor interpretability and high computational cost in large samples or high-dimensional settings (Muandet et al., 2017; Park et al., 2021); neural network-based methods (Holovchak et al., 2025) that enjoy model flexibility, yet not allowing user-specified causal quantities; and Bayesian methods (Venturini et al., 2015; Xu et al., 2018) that often incur heavy computational costs. Overall, these methods struggle to balance flexibility, interpretability, and computational efficiency.

Fregression bridges this gap through its modular, variation independent parameterization and distributional regression models, which directly targets specific distributional quantities while preserving both transparency and efficiency in estimation and data simulation.

1.2.4 Generative models for causal data simulation

Several generative models have been proposed to simulate realistic data for benchmarking causal inference methods. Athey et al. (2024) introduced a Monte Carlo simulation framework using Wasserstein Generative Adversarial Networks (GANs) to benchmark causal models and estimators. Similarly, Neal et al. (2020) developed RealCause, which builds on neural autoregressive flows (Huang et al., 2018). Parikh et al. (2022) proposed Credence, a deep generative model based on variational autoencoders that represents the joint distribution by separately modelling the marginal distribution of covariates, the treatment assignment given covariates, and the outcome distribution conditional on covariates and treatments. The conditional and marginal outcome distributions are only indirectly specified through a post hoc optimization step embedded in the training loss, and the model is limited to binary treatments.

None of these methods allows for direct control over the marginal causal effect. Frugal flows (de Vassimon Manela et al., 2024) tackle the challenges above by incorporating the frugal parameterization into normalizing flows, to directly model the marginal interventional distribution. However, reliance on copula flows (Kamthe et al., 2021) restricts them to univariate outcomes or static regimes, demands hierarchical copulas for multivariate outputs, and exhibits sensitivity to hyperparameters.

Compared to density estimation based generative models that are restricted to invertible transformations (such as frugal flows and RealCause, that rely on normalizing flows) and tractable decoder distributions (for example, CausalEGM, CEVAE and Credence that build on variational autoencoders, normally relying on Gaussian or Bernoulli decoders), fregression is easier to fit and allows direct control of causal margin without inflating complexity, thereby providing robust, tractable data simulation.

1.3 Structure

The fregression method is proposed in Section 2, we introduce the architecture in Section 2.3, and we present the estimation procedure and identifiability results in Section 2.4. We provide consistency results for fitting the model in Section 3. Fregression exhibits strength with respect to treatment extrapolation, which is explored in Section 4. Its flexibility for longitudinal data and survival analysis is demonstrated in Section 5. We then provide empirical results to show fregression’s comprehensive capability in synthetic experiments (Section 6) and real trial data LEADER (Section 7). We conclude the paper with Section 8 with potential further directions.

2 Method

In this section we describe the necessary notation and basic method for fregression.

2.1 Notations

We use a hat to mark the samples generated from a (fitted) fregression model, for instance, \hat{Z} , \hat{X} , or \hat{Y} . The Euclidean norm of a vector $x \in \mathbb{R}^d$ is denoted $\|x\|$. We use \mathbb{P}_V to denote the distribution of a random variable V , p_V for the corresponding density or mass function, \mathbb{P}^n for the empirical measure, and $P(A)$, $A \subseteq \Omega$ to denote the probability of an event A . Expectations are represented by \mathbb{E} , so $\mathbb{E}f = \int f d\mathbb{P}$. We use \bar{W}_k to denote (W_0, \dots, W_k) , the time-varying variable W ’s values up to the time point k . As with the frugal parameterization (Evans and Didelez 2024, Remark 1.4), our method fits within any causal inference framework, including Pearl’s ‘*do*(.)’ operator $P(Y = y | \text{do}(X = x))$. For convenience, in this paper we follow the potential outcomes framework (Neyman 1923 and Rubin 1974), where we write the outcome under a treatment $x \in \mathcal{X}$ as $Y(x)$ and its distribution is denoted $\mathbb{P}_{Y(x)}$. As noted in Section 1, $\mathbb{P}_{Y(x)}$ is equivalent to $\mathbb{P}_{Y|X=x}^*$.

In this paper, we consider a general setting depicted in Figure 1(a), which describes a simple time-varying confounding scenario. We partition the treatment vector $X = (X_0, X_1)$, where X_0 denotes the intervention on the treatments causally prior to Z , and X_1 denotes interventions on the treatments causally subsequent to Z ; the respective supports are \mathcal{X}_0 and \mathcal{X}_1 . In such a setting, when we write $Y(x)$, it is equivalent to $Y(x_0, x_1)$. This structure is commonly seen in longitudinal analysis (Havercroft and Didelez, 2012) and serves as the motivating example for simulating data that satisfies marginal requirements in Evans and Didelez (2024). In the absence of any interventions on the covariates, the causal DAG reduces to the simpler form shown in Figure 1(b), which is more typical in static settings.

2.2 Review of Key Concepts

We have provided a brief review of the frugal parameterization in the introduction. As hinted by its name, fregression employs egression as the generative model. Before we proceed further to more details, we provide a review of concepts related to egression here.

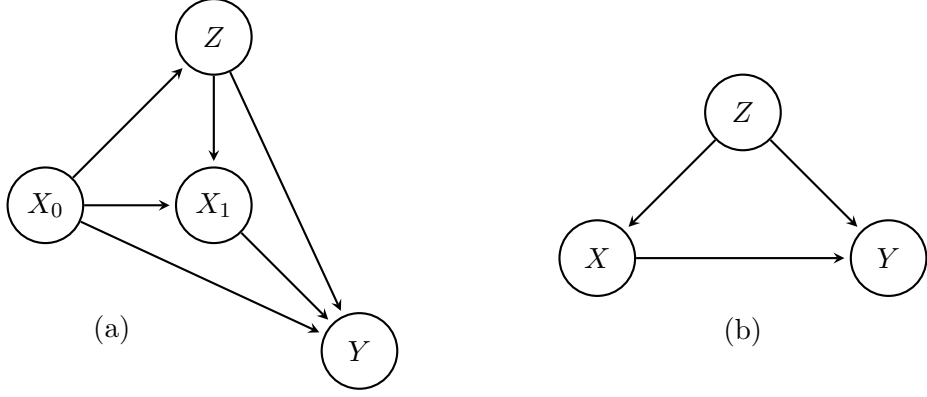


Figure 1: (a) General causal DAG considered in this paper. This time-dependent confounding structure is commonly seen in longitudinal data. (b) Causal DAG without X_0 . This structure is more common in time-fixed settings.

Parameterized by a neural network, engression aims to estimate the full conditional distribution of a response Y given predictors W . This predictive distribution $Y | W = w$ can be taken from a general model class produced by engression and be written as $\mathcal{M} = \{f(w, \zeta)\}$, where $f : (w, \zeta) \mapsto y$ belongs to a function class and ζ is a random vector with a pre-specified distribution, independent of the covariates. A typical choice is that ζ follows the multivariate standard Gaussian distribution. We write $\mathbb{P}_f(y | w)$ for the distribution of $f(w, \zeta)$, with the randomness coming from ζ , and $\mathcal{L}(\mathbb{P}, \mathbb{P}_0)$ for the loss function of a distribution \mathbb{P} given a reference \mathbb{P}_0 . Engression specifically concerns a solution to:

$$\tilde{f} = \underset{f \in \mathcal{M}}{\operatorname{argmin}} \mathbb{E}_{(Y, W) \sim \mathbb{P}} \mathcal{L}(\mathbb{P}_f(y | W), Y).$$

Although different loss functions can be used in engression (Shen and Meinshausen, 2024, Appendix D), it shows stable, robust performance using the energy loss $\mathcal{L}(-\operatorname{ES}(\mathbb{P}_f(y | W), Y))$, where the energy score (ES) is defined as

$$\operatorname{ES}(\mathbb{P}, u) = \frac{1}{2} \mathbb{E}_{U, U' \sim \mathbb{P}} \|U - U'\| - \mathbb{E}_{U \sim \mathbb{P}} \|U - u\| \quad (1)$$

given a distribution \mathbb{P} and an observation u (Gneiting and Raftery, 2007); the U, U' are taken to be independent. The energy score is associated with the energy distance (Székely and Rizzo, 2013), a distributional divergence that is defined as

$$\operatorname{ED}(\mathbb{P}, \mathbb{P}') = 2\mathbb{E}_{U \sim \mathbb{P}, V \sim \mathbb{P}'} \|U - V\| - \mathbb{E}_{U, U' \sim \mathbb{P}} \|U - U'\| - \mathbb{E}_{V, V' \sim \mathbb{P}'} \|V - V'\|. \quad (2)$$

This is a special case of the squared maximum mean discrepancy (MMD) distance, denoted by $\operatorname{MMD}^2(\mathbb{P}, \mathbb{P}')$, with kernel $k(u, v) = \frac{1}{2}(\|u\| + \|v\| - \|u - v\|)$ (Sejdinovic et al., 2013). Using energy loss provides computational simplicity: the estimation of the score or distance is explicitly computed based on sampling. Since the energy distance differs from the energy loss only by a positive scaling plus an additive constant that does not depend on the generator parameters, minimizing the energy distance yields the same fitted generator as minimizing the energy loss. For compatibility with the relevant literature regarding distributional distance (Briol et al., 2019), we prove the consistency of models trained aiming at minimizing energy distance $\operatorname{ED}(\mathbb{P}_f, \mathbb{P})$ in Section 3.

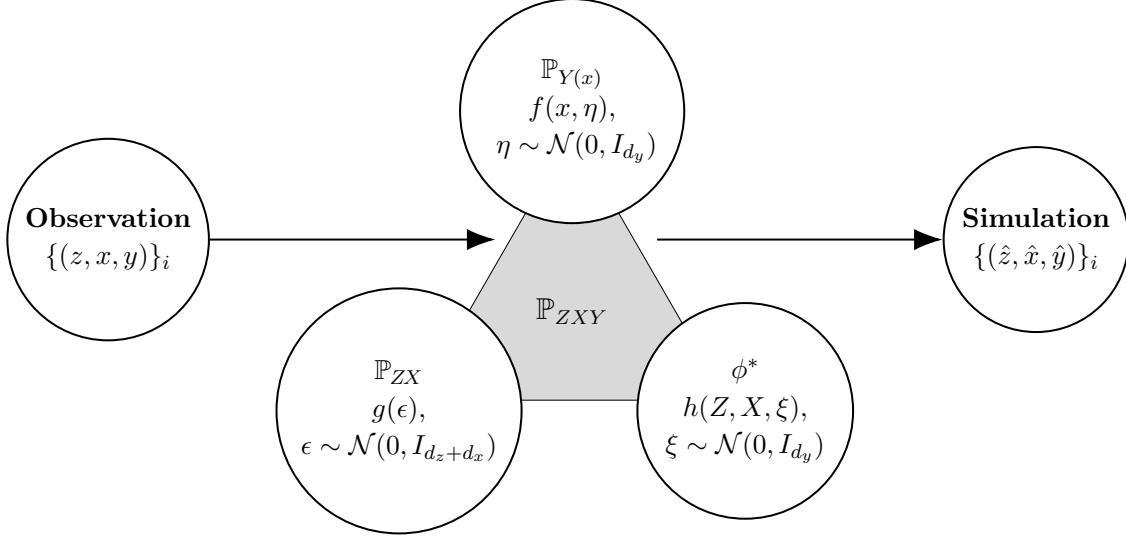


Figure 2: Estimation and simulation architecture of fregression.

Another speciality of engression is that its model class \mathcal{M} contains the pre-additive noise models (pre-ANMs). Define function classes \mathcal{F} and \mathcal{G} . The pre-ANMs can be written as

$$f(w + g(\zeta)) : f \in \mathcal{F}, g \in \mathcal{G}, \quad (3)$$

where $g(\zeta)$ represents the pre-additive noise; f and g are to be learned. Shen and Meinshausen (2024) provided detailed discussions on the extrapolation properties provided by pre-ANMs, allowing one to relax the causal effect identification assumptions; details are given in Section 4.

2.3 Model and Parametrization

The architecture of fregression is shown in Figure 2. A fregression model contains three components, each corresponding to one component in the frugal parameterization:

- For the joint distribution \mathbb{P}_{ZX} , we build a generative model:

$$g(\epsilon), \quad (4)$$

where $\epsilon \sim \mathcal{N}(0, I_{d_z+d_x})$ and $g : \mathbb{R}^{d_z+d_x} \rightarrow \mathbb{R}^{d_z+d_x}$.

- Given a specified form of the (marginal) causal effect $\mathbb{P}_{Y(x)}$, we use

$$Y = f(x, \eta) \quad (5)$$

as the generative form, where $\eta \sim \mathcal{N}(0, I_{d_y})$. For example, if $\mathbb{P}_{Y(x)}$ is $\mathcal{N}(x, 1)$, it can be specified in a generative form as $f(x, \eta) = x + \eta$.

- Association remainder $\phi_{Y|ZX}^*$. Given the causal margin in (5), the remaining part to fully specify the distribution $\mathbb{P}_{Y|ZX}$ is a conditional distribution of $\eta | Z = z, X = x$. For this, we build a conditional generative model

$$\tilde{\eta} = h(z, x, \xi), \quad (6)$$

where $\xi \sim \mathcal{N}(0, I_{d_y})$. Similar to the copula measure chosen by the original frugal parameterization, this term captures the association between Y and (Z, X) in a way that is compatible with the specified causal margin.

Frengression parameterizes the joint (observed) distribution via generative models, preserving the same properties as the original frugal parametrization. First, the three components jointly specify the whole distribution \mathbb{P}_{ZXY} . To see this, note that model (4) specifies the distribution for (Z, X) , while models (5) and (6) together specify a distribution of $Y | Z, X$. Furthermore, the three components can be chosen to be variation independent. The first component is about the distribution of (Z, X) whereas in the other two components, X and Z are either given or conditioned on; thus, g is variation independent of (f, h) . Note that the marginal distribution of η is always fixed as the standard Gaussian and is thus not a model component. For the variation independence between f and h , note that model (5) specifies the causal margin $\mathbb{P}_{Y(x)}$ only through the function f with a fixed value of x and η drawn from its (fixed) marginal distribution, whereas model (6) is about the conditional distribution of $\eta | Z, X$ with a constraint of a normal margin. Thus, these two components are variation independent. More details are given in Remark 2.1.

We write a frengression model as $\varphi = (g, f, h)$. While we specify the distributions of ϵ , η and ξ in this paper, their distributions can be non-Gaussian, provided that they are sampled independently of the observed data. Note that even though we draw η from a standard normal distribution, because it is subsequently passed through the non-linear function $f(\cdot)$, the interventional distribution induced by frengression need not be Gaussian.

Remark 2.1 (Interventional distribution $\mathbb{P}_{Y(x)}$ versus conditional distribution $\mathbb{P}_{Y|X=x}$). Model (5) with a fixed x and η following its marginal distribution induces the interventional distribution of $\mathbb{P}_{Y(x)}$, whereas model (5) in combination with (6), that is $f(X, h(Z, X, \xi))$, induces the conditional distribution of $\mathbb{P}_{Y|ZX}$. Note that in the latter case, X and the noise term $h(Z, X, \xi)$ are correlated, whereas in the ‘marginal generative causal model’ (5), x is fixed and so is independent from the noise term η .

Remark 2.2 (Privacy). Our generative framework factorizes the simulation process into three variation-independent modules, so each can be specified or replaced on its own. In contexts where the variables Z or X contain sensitive information, the model to generate them ($g(\cdot)$) can be replaced by any differentially private generative mechanism. By the post-processing theorem of differential privacy (Dwork et al., 2006), any further mapping applied to a differentially private algorithm remains differentially private. The entire simulated dataset also preserves that privacy guarantee, making our approach naturally extendable to privacy-sensitive settings.

2.4 Estimation

As in engression, parameters of each component in frengression are typically estimated by minimizing the energy loss, for its simplicity and convenience. However, other loss functions can be used, such as KL divergence.

On the population level, the objective function for model (4) is

$$\mathcal{L}_{ZX}(g) := \mathcal{L}(\mathbb{P}_{ZX}, \mathbb{P}_g) = \mathbb{E} \left[\|(Z, X) - g(\epsilon)\| - \frac{1}{2} \|g(\epsilon) - g(\epsilon')\| \right]. \quad (7)$$

The objective for models (5) and (6) jointly is

$$\mathcal{L}_{Y|ZX}(f, h) := \mathbb{E} \left[\|Y - f(X, \tilde{\eta})\| - \frac{1}{2} \|f(X, \tilde{\eta}) - f(X, \tilde{\eta}')\| \right] + \mathbb{E} \left[\|\eta - \bar{\eta}\| - \frac{1}{2} \|\bar{\eta} - \bar{\eta}'\| \right], \quad (8)$$

where $\tilde{\eta} = h(Z, X, \xi)$, $\tilde{\eta}' = h(Z, X, \xi')$, $\bar{\eta} = h(\bar{Z}, \bar{X}, \xi'')$, and $\bar{\eta}' = h(\bar{Z}', \bar{X}, \xi''')$ with $\eta \sim \mathcal{N}(0, I_{d_y})$, $\xi, \xi', \xi'', \xi''' \stackrel{\text{i.i.d.}}{\sim} \mathcal{N}(0, I_{d_y})$, $(Z, X) \sim \mathbb{P}_{ZX}$, $\bar{X} \sim \mathbb{P}_X$ and $\bar{Z}, \bar{Z}' \stackrel{\text{i.i.d.}}{\sim} \mathbb{P}_{Z|X_0}$. This is chosen because these two models should be estimated such that:

- the object $f(X, \tilde{\eta})$, when $\tilde{\eta}$ is drawn from its conditional distribution given (Z, X) , matches the observed conditional distribution $\mathbb{P}_{Y|ZX}$, which is ensured by the first term in (8);
- the interventional distribution of $\tilde{\eta}(x)$ is the standard normal, as chosen by us, for any x .

As for sampling from $\mathbb{P}_{Z|X_0}$, if X_0 does not exist (i.e. the confounder Z is not affected by any treatment as in Figure 1(b)), we do it independently from the marginal distribution \mathbb{P}_Z ; otherwise, we need to learn an auxiliary model $e^*(x_0, \zeta)$ that matches the distribution of $\mathbb{P}_{Z|X_0}$ via the standard engression approach

$$e^* \in \operatorname{argmin}_e \mathbb{E} \left[\|Z - e(X_0, \zeta)\| - \frac{1}{2} \|e(X_0, \zeta) - e(X_0, \zeta')\| \right],$$

where $\zeta, \zeta' \stackrel{\text{i.i.d.}}{\sim} \mathcal{N}(0, I_{d_z})$.

We define the population version of fregression, denoted by $\varphi^* = (g^*, f^*, h^*)$, as the solution to minimizing the objective functions:

$$\begin{aligned} g^* &= \operatorname{argmin}_g \mathcal{L}_{ZX}(g) \\ (f^*, h^*) &= \operatorname{argmin}_{f, h} \mathcal{L}_{Y|ZX}(f, h). \end{aligned}$$

To show the population guarantees that fregression learns each component correctly and recovers the true data generating process of (Z, X, Y) , we impose the following assumptions:

Assumption 2.1 (Correct specification). *We write the function classes $\mathcal{G} = \{g(\epsilon)\}$, $\mathcal{F} = \{f(x, \eta)\}$, and $\mathcal{H} = \{h(z, x, \xi)\}$. There exist $g' \in \mathcal{G}$, $f' \in \mathcal{F}$, and $h' \in \mathcal{H}$ such that $g'(\epsilon) \sim \mathbb{P}_{ZX}$ with $\epsilon \sim \mathcal{N}(0, I_{d_x+d_z})$, $f'(x, \eta) \sim \mathbb{P}_{Y(x)}$ with $\eta \sim \mathcal{N}(0, I_{d_y})$ and $f'(x, h'(z, x, \xi)) \sim \mathbb{P}_{Y|Z=z, X=x}$ with $\xi \sim \mathcal{N}(0, I_{d_y})$.*

Assumption 2.2 (Identification assumptions regarding DAG in Figure 1(a)).

(i) **Positivity:** The joint support of (X_0, Z, X_1) is full, that is,

$$p_{X_0ZX_1}(x_0, z, x_1) > 0$$

for almost all $(x_0, z, x_1) \in \mathcal{X}_0 \times \mathcal{Z} \times \mathcal{X}_1$.

(ii) **Unconfoundedness:** The potential outcome $Y(x)$ is independent of the observed treatment given past covariates and treatment:

$$Y(x) \perp\!\!\!\perp X_1 \mid Z = z, X_0 = x_0 \text{ and } Y(x) \perp\!\!\!\perp X_0, \quad \forall x \in \mathcal{X}.$$

(iii) **Consistency:** If $X = x$ then the observed outcome equals the potential outcome at that level:

$$X = x \implies Y = Y(x), \quad \forall x \in \mathcal{X}.$$

When the conditions in Assumption 2.2 hold, we have that the potential outcome distribution $\mathbb{P}_{Y(x)}$ is identifiable from the observed joint distribution of (Z, X, Y) in Figure 1(a):

Proposition 2.1 (Identifiability). *When Assumption 2.2 is satisfied, we have:*

$$p_{Y(x)}(y) = \int_{\mathcal{Z}} p_{Y|X_0ZX_1}(y | x_0, z, x_1) p_{Z|X_0}(z | x_0) dz.$$

The proof can be found in Appendix A.1. We later show in Section 4 that the positivity assumption can be relaxed by the nice extrapolation properties of pre-ANMs.

Assumption 2.1 asserts the existence of functions (g', f', h') , while Assumption 2.2 guarantees unique potential outcome distributions. With these assumptions, we introduce the following proposition, which provides the population guarantee that frengression correctly learns the true distributions when the model is correctly specified.

Proposition 2.2 (Correctness). *When Assumptions 2.1 and 2.2 hold, the frengression solution $\varphi^* = (g^*, f^*, h^*)$ satisfies the following: for all $x \in \mathcal{X}$ and $z \in \mathcal{Z}$,*

$$\begin{aligned} g^*(\epsilon) &\sim \mathbb{P}_{ZX} \\ f^*(x, \eta) &\sim \mathbb{P}_{Y(x)} \\ f^*(x, h^*(z, x, \xi)) &\sim \mathbb{P}_{Y|Z=z, X=x}, \end{aligned}$$

where $\epsilon \sim \mathcal{N}(0, I_{d_z+d_x})$, $\eta \sim \mathcal{N}(0, I_{d_y})$, and $\xi \sim \mathcal{N}(0, I_{d_y})$.

The proof of Proposition 2.2 is provided in Appendix A.2.

2.4.1 Finite-sample Frengression

φ^* solves the population objectives in (7) and (8). In practice, we only have access to finite samples $\{(Z_i, X_i, Y_i)\}_{i=1}^n \sim \mathbb{P}_{ZXY}(z, x, y)$; the empirical version of frengression is

$$\begin{aligned} \hat{g} &= \underset{g}{\operatorname{argmin}} \hat{\mathcal{L}}_{ZX}(g) \\ (\hat{f}, \hat{h}) &= \underset{f, h}{\operatorname{argmin}} \hat{\mathcal{L}}_{Y|ZX}(f, h), \end{aligned}$$

where the finite sample loss function estimates are

$$\hat{\mathcal{L}}_{ZX}(g) := \frac{1}{n} \sum_{i=1}^n \left[\frac{1}{m} \sum_{j=1}^m \|(X_i, Z_i) - g(\epsilon_{i,j})\| - \frac{1}{2m(m-1)} \sum_{j=1}^m \sum_{\substack{j'=1 \\ j' \neq j}}^m \|g(\epsilon_{i,j}) - g(\epsilon_{i,j'})\| \right], \quad (9)$$

$$\begin{aligned}
\hat{\mathcal{L}}_{Y|ZX}(f, h) := & \frac{1}{n} \sum_{i=1}^n \left[\frac{1}{m} \sum_{j=1}^m \|Y_i - f(X_i, \tilde{\eta}_{i,j})\| - \frac{1}{2m(m-1)} \sum_{j=1}^m \sum_{\substack{k=1 \\ k \neq j}}^m \|f(X_i, \tilde{\eta}_{i,j}) - f(X_i, \tilde{\eta}_{i,k})\| \right] \\
& + \frac{1}{n} \sum_{i=1}^n \left[\frac{1}{m} \sum_{j=1}^m \|\eta_i - \bar{\eta}_{i,j}\| - \frac{1}{2m(m-1)} \sum_{j=1}^m \sum_{\substack{k=1 \\ k \neq j}}^m \|\bar{\eta}_{i,j} - \bar{\eta}_{i,k}\| \right], \tag{10}
\end{aligned}$$

respectively. Here, for $i = 1, \dots, n$, $l = 1, \dots, m$, we simulate $\epsilon_{i,l} \sim \mathcal{N}(0, I_{d_z+d_x})$, $\eta_{i,l} \sim \mathcal{N}(0, I_{d_y})$, and obtain $\tilde{\eta}_{i,l} = h(Z_i, X_i, \xi_{i,l})$, $\bar{\eta}_{i,k} = h(Z'_i, X_i, \xi_{i,k})$, with $\xi_{i,l} \sim \mathcal{N}(0, I_{d_y})$, where Z'_i is either drawn from a random permutation of the observed data or from the auxiliary model e . The empirical version of auxiliary model e can be fitted by minimizing

$$\hat{\mathcal{L}}_{Z|X_0}(e) := \frac{1}{n} \sum_{i=1}^n \left[\frac{1}{m} \sum_{j=1}^m \|Z_i - e(X_i, \zeta_{i,j})\| - \frac{1}{2m(m-1)} \sum_{j=1}^m \sum_{\substack{j'=1 \\ j' \neq j}}^m \|e(X_i, \zeta_{i,j}) - e(X_i, \zeta_{i,j'})\| \right], \tag{11}$$

where $\zeta_{i,l} \sim \mathcal{N}(0, I_{d_z})$, for $i = 1, \dots, n$, $l = 1, \dots, m$.

Equations (9)–(11) are unbiased estimators of the population objectives. In Section 3, we present theoretical guarantees that by optimizing finite-sample empirical losses, the model parameters converge asymptotically to the value that minimizes the divergence between the generative distribution and the target distribution.

In practice, we parameterize g , f and h with neural networks. The resulting empirical objectives are therefore almost everywhere differentiable with respect to every model parameter, allowing us to optimize them with stochastic gradient descent to obtain the fitted fregression model.

2.5 Sampling

Given the generative nature of our model, sampling from a fitted fregression is straightforward. We provide the sampling procedures from the population version φ^* for four common simulation scenarios below:

1. Simulate (\hat{Z}, \hat{X}) .
Sample $\epsilon \sim \mathcal{N}(0, I_{d_z+d_x})$ and set $(\hat{Z}, \hat{X}) = g^*(\epsilon)$.
2. Simulate $\hat{Y}(x)$.
For a treatment value x , draw $\eta \sim \mathcal{N}(0, I_{d_y})$ and compute $\hat{Y}(x) = f^*(x, \eta)$.
3. Simulate $(\hat{Z}, \hat{X}, \hat{Y})$ from the joint distribution of (Z, X, Y) .
 - (i) Generate (\hat{Z}, \hat{X}) as in step 1.
 - (ii) Draw $\xi \sim \mathcal{N}(0, I_{d_y})$ and obtain $\tilde{\eta} = h^*(\hat{Z}, \hat{X}, \xi)$.
 - (iii) Produce the response via $\hat{Y} = f^*(\hat{X}, \tilde{\eta})$.
4. Simulate $(\hat{Z}, \hat{X}, \hat{Y}(x'))$ from full single world intervention graphs distributions (SWIGs, Richardson and Robins, 2013):
 - (i) Generate (\hat{Z}, \hat{X}) and obtain $\tilde{\eta} = h^*(\hat{Z}, \hat{X}, \xi)$.

- (ii) Produce the response via $f^*(x', \tilde{\eta})$ with a specified x' .

The (g^*, f^*, h^*) can be replaced by model $(\hat{g}, \hat{f}, \hat{h})$ fitted using finite samples. Taken together, these sampling schemes allow us to generate synthetic observations from any component or the full joint distribution of a model fitted on real data.

2.6 Sampling-based inference

Fregression allows sampling-based inference. For instance, a typical quantity of interest is the average potential outcome $\mathbb{E}Y(x)$ under a specific intervention x . A fitted fregression model contains $\hat{f}(x, \eta)$, and this estimates the marginal outcome distribution. Thus, for any given intervention value x , we sample $\eta_i \sim \mathcal{N}(0, I_{d_y})$ for $i = 1, \dots, m$. Then we obtain a sample $\{Y_i = \hat{f}(x, \eta_i), i = 1, \dots, m\}$ from the estimated distribution $\hat{\mathbb{P}}_{Y(x)}$. The expected potential outcome can thus be estimated using the empirical mean $\frac{1}{m} \sum_{i=1}^m \hat{f}(x, \eta_i)$. Besides the interventional mean, any other quantity can also be estimated; for instance, the α -quantile of $\mathbb{P}_{Y(x)}$ is consistently estimated by the α -quantile of this sample.

3 Model Consistency

In this section we provide a general consistency result for generative modelling with finite sample-based energy distance as the loss function. We write the generative model as g_θ , which is parameterized by $\theta \in \Theta$ to learn an unknown data generating distribution \mathbb{Q} . We denote the probability measure produced by the generative model by \mathbb{P}_θ . Given that fregression is parameterized using a neural network, θ is the collection of neural network weights.

In this paper, we train the generative model g_θ by minimizing the energy distance between \mathbb{P}_θ and \mathbb{Q} . Following the definition in (2), we write the population energy distance as

$$\text{ED}(\mathbb{P}_\theta, \mathbb{Q}) = 2\mathbb{E}_{X \sim \mathbb{P}_\theta, Y \sim \mathbb{Q}} \|X - Y\| - \mathbb{E}_{X, X' \sim \mathbb{P}_\theta} \|X - X'\| - \mathbb{E}_{Y, Y' \sim \mathbb{Q}} \|Y - Y'\|. \quad (12)$$

We make the following assumption:

Assumption 3.1 (Existence of θ^*). *We assume there exists a unique minimizer*

$$\theta^* = \arg \min_{\theta \in \Theta} \text{ED}(\mathbb{P}_\theta, \mathbb{Q}).$$

θ^* is what we would like to estimate if it exists, as $\mathbb{P}_{\theta^*} \in \{\mathbb{P}_\theta, \theta \in \Theta\}$ is the ‘closest’ distribution to \mathbb{Q} generated by g_θ .

In practice, it is not common to have direct access to \mathbb{Q} ; instead, we generally have access to empirical observations from \mathbb{Q} : $\{y_1, \dots, y_n\}$, forming the empirical measure $\mathbb{Q}^n = \frac{1}{n} \sum_{i=1}^n \delta_{y_i}$. When g_θ is analytically accessible, an estimator could be found as

$$\hat{\theta}_n = \arg \min_{\theta \in \Theta} \text{ED}(\mathbb{P}_\theta, \mathbb{Q}^n),$$

where

$$\text{ED}(\mathbb{P}_\theta, \mathbb{Q}^n) = \frac{2}{n} \sum_{j=1}^n \mathbb{E}_{X \sim \mathbb{P}_\theta} \|X - y_j\| - \mathbb{E}_{X, X' \sim \mathbb{P}_\theta} \|X - X'\| - \frac{1}{n(n-1)} \sum_{j=1}^n \sum_{\substack{j'=1 \\ j \neq j'}}^n \|y_j - y_{j'}\|.$$

If g_θ is not directly accessible, but samples can be independently drawn from it, the estimator then becomes

$$\hat{\theta}_{m,n} = \arg \min_{\theta \in \Theta} \text{ED}(\mathbb{P}_\theta^m, \mathbb{Q}^n),$$

where

$$\text{ED}(\mathbb{P}_\theta^m, \mathbb{Q}^n) = \frac{2}{nm} \sum_{i=1}^m \sum_{j=1}^n \|x_i - y_j\| - \frac{1}{m(m-1)} \sum_{i=1}^m \sum_{\substack{i'=1 \\ i' \neq i}}^m \|x_i - x_{i'}\| - \frac{1}{n(n-1)} \sum_{j=1}^n \sum_{\substack{j'=1 \\ j \neq j'}}^n \|y_j - y_{j'}\|.$$

$\text{ED}(\mathbb{P}_\theta^m, \mathbb{Q}^n)$ aligns with the finite-sample objective functions defined in Section 2.4.1.

Under the assumption that the minimizer $\theta^* = \arg \min_{\theta \in \Theta} \text{MMD}(\mathbb{P}_\theta, \mathbb{Q})$ exists, Briol et al. (2019) proved the consistency of $\hat{\theta}_n$ and $\hat{\theta}_{m,n}$, i.e. $\lim_{n \rightarrow \infty} \hat{\theta}_n = \theta^*$ and $\lim_{m,n \rightarrow \infty} \hat{\theta}_{m,n} = \theta^*$, when the kernel used in the MMD is bounded. However, fregression is trained using energy distance, which is a special case of MMD employing an unbounded, Euclidean distance-based kernel. Although it is reasonable to argue that a bounded covariate space may lead to a bounded kernel in practice, our goal is to extend the theoretical results of Briol et al. to cover the unbounded kernels used in energy distance that possess finite moments. Here we provide the consistency result under the following alternative two assumptions.

Assumption 3.2 (Sub-exponential tails). *There exist constants $C, \alpha > 0$ such that*

$$P(\|X\| > t) \leq C \exp(-\alpha t), \quad \forall t > 0,$$

for $X \sim \mathbb{P}_\theta, \forall \theta \in \Theta$ and $X \sim \mathbb{Q}$.

Assumption 3.3 (Finite second moment). *There exists a constant $M > 0$ such that*

$$\mathbb{E}_{\mathbb{P}_\theta} \|X\|^2 \leq M^2 \quad \text{and} \quad \mathbb{E}_{\mathbb{Q}} \|X\|^2 \leq M^2.$$

We now introduce the consistency result:

Theorem 3.1 (Consistency). *Suppose Assumptions 3.1–3.3 hold. Then*

$$\hat{\theta}_n \xrightarrow[n \rightarrow \infty]{a.s.} \theta^* \quad \text{and} \quad \hat{\theta}_{m,n} \xrightarrow[m,n \rightarrow \infty]{a.s.} \theta^*.$$

Theorem 3.1 shows that, as the sample sizes m, n go to infinity, a fitted fregression converges to the generative model under which the distribution sampled is closest to the ground truth generating distribution \mathbb{Q} . If further, Assumption 2.1 holds, i.e. $\mathbb{Q} \in \{\mathbb{P}_\theta, \theta \in \Theta\}$, then the distribution generated by fregression converges to the true distribution. The proof is provided in Appendix A.3.

4 Extrapolation

For simplicity, in this section, we consider the case with univariate treatment X and outcome Y but allow for multiple covariates Z .

Assumption 4.1 (Pre-ANM). *The causal margin can be parametrized via a pre-additive noise model*

$$Y = \tilde{f}(X + \tilde{\eta}),$$

where \tilde{f} is any strictly monotone function and $\tilde{\eta}$ can follow any continuous distribution and is independent of X . Without loss of generality, assume $\tilde{\eta}$ has a median 0 and is supported on $[-\tilde{\eta}_0, \tilde{\eta}_0]$ for some $\tilde{\eta}_0 > 0$; we let $\tilde{\eta}_0 = \infty$ when $\tilde{\eta}$ has an unbounded support.

This assumption holds, for example, when the structural equation of Y is given by $Y = \tilde{f}(X + \tilde{h}(Z, \tilde{\xi}))$, where \tilde{h} is any bivariate function taking both Z and $\tilde{\xi}$ as arguments, the noise $\tilde{\xi} \sim \mathcal{N}(0, 1)$ can be correlated with X , and when the treatment does not causally affect the covariates.

We study the extrapolation performance of fregression for median estimation of the causal margin. Let $\tilde{m}(x)$ denote the true median of $Y(x)$ for any x . When Assumption 4.1 holds, the fregression model class can be smaller for Assumption 2.1 to hold. Specifically, we reparametrize the model for the causal margin as $f(X + f_1(\eta))$, where f and f_1 are both strictly monotone functions. Denote the median of the population fregression solution as $m^*(x)$, which is defined as the median of $f^*(x, \eta)$.

The following proposition indicates that fregression can recover the true median of causal margin for x outside of the support. The proof can be found in Appendix A.4.

Proposition 4.1 (Extrapolation). *Let the support of X be $\mathcal{X} = [x_{\min}, x_{\max}]$. Under Assumption 4.1, we have*

$$m^*(x) = \tilde{m}(x)$$

for all $x \in [x_{\min} - \tilde{\eta}_0, x_{\max} + \tilde{\eta}_0]$.

The experimental results provided in Figure 4 show that fregression maintains accurate estimates even when extrapolating beyond the observed values of treatment X .

5 Fregression on Sequential Data

The discussion in Sections 2 and 3 introduced the basic fregression machinery in the static case. Many scientific questions, however, involve time-varying decision points, such as longitudinal studies and survival analysis, where treatment decisions may change over time in response to evolving patient histories. The frugal parameterization is particularly helpful in longitudinal analysis, as the time-varying covariates are marginalized out. Leveraging this idea, especially the recursive/nested variant of frugal parameterization introduced in Section 6 of Evans and Didelez (2024), fregression extends naturally to the longitudinal context.

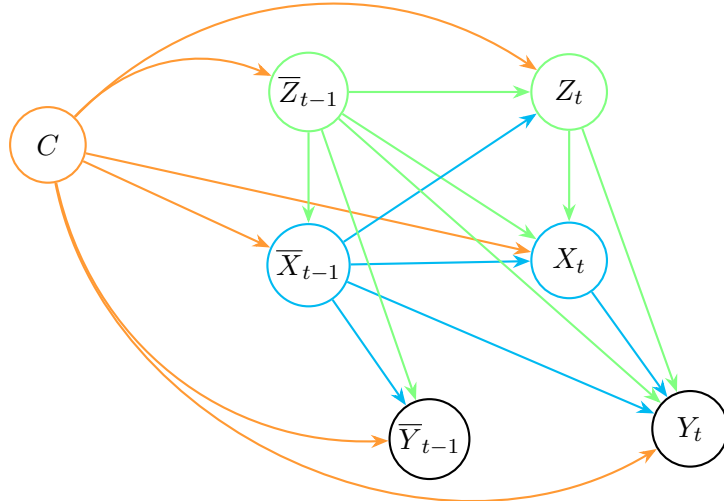


Figure 3: Example diagram of longitudinal data. For simplicity we present one time point t as an example, and we show that (Z_t, X_t, Y_t) are connected with all previous time steps. As with the static case, there are no dimensional constraints on the variables.

An illustrative causal diagram is given in Figure 3. Let $C \in \mathbb{R}^{d_c}$ denote the static, pre-treatment baseline covariates; for the ease of notation, we use Z , X , Y to denote the vector: $Z = (Z_0, \dots, Z_{T-1})$ with $Z_t \in \mathbb{R}^{d_z}$ the time-varying covariates; $X = (X_0, \dots, X_{T-1})$, with $X_t \in \mathbb{R}^{d_x}$ the sequence of interventions; and $Y = (Y_0, \dots, Y_{T-1})$, $Y_t \in \mathbb{R}^{d_y}$ the observed outcomes. In the special case of survival-valued outcomes, $Y_t \in \{0, 1\}$ with $Y_t = 1$ indicating an event occurrence; simulation stops after such an event. Other than survival variables, all can assume continuous or discrete values.

5.1 Model

We illustrate the following sections with an example where the interventional distribution of interest is $\mathbb{P}_{Y(x)|C}$.

For data as described above, we write the sequential fregression as φ_s . We first build a model to generate the baseline covariates C using the unconditional egression $g_c(\varsigma)$, where $\varsigma \sim \mathcal{N}(0, I_{d_c})$. Then we build the sequential fregression $(\varphi_0, \dots, \varphi_{T-1})$, where $\varphi_t = (g_t, f_t, h_t)$ for $t = 0, \dots, T-1$. For each $t \in \{0, \dots, T-1\}$:

- When $t = 0$, build $g_0(c, \epsilon)$ for the joint distribution $\mathbb{P}_{Z_0 X_0 | C}$; otherwise $g_t(c, \bar{z}_{t-1}, \bar{x}_{t-1}, \epsilon)$ for the joint distribution $\mathbb{P}_{Z_t X_t | C \bar{Z}_{t-1} \bar{X}_{t-1}}$. In both cases, $\epsilon \sim \mathcal{N}(0, I_{d_z + d_x})$.
- $Y = f_t(c, \bar{x}_t, \eta)$, $\eta \sim \mathcal{N}(0, I_{d_y})$ for the interventional distribution $\mathbb{P}_{Y_t(\bar{x}_t)|C}$ of treatment values up to time t given baseline covariates C .

- $\tilde{\eta} = h_t(c, \bar{z}_t, \bar{x}_t, \xi)$ where $\xi \sim \mathcal{N}(0, I_{d_y})$; this term is used for modelling the association.

The sequential fregression consists of all the components above: $\varphi_s = (g_c(\zeta), \varphi_0, \varphi_1, \dots, \varphi_{T-1})$. For convenience, we also denote $g = (g_0, \dots, g_{T-1})$, $f = (f_0, \dots, f_{T-1})$ and $h = (h_0, \dots, h_{T-1})$, then φ_s can also be expressed as $\varphi_s = (g_c, g, f, h)$.

For longitudinal settings we introduce two variants of fregression, *FregressionSeq* and *FregressionSurv*. Both inherit the modelling architecture described above; the distinction is that *FregressionSurv* is tailored to survival data, where the effective sample size shrinks over time as events occur. Accordingly, each φ_t is trained on the subpopulation that still at risk at time t . This renormalization does not affect the generative procedure, because at simulation time we censor a synthetic trajectory as soon as an event occurs and remove it from all subsequent steps, ensuring that the simulated data follow the same at-risk pattern as the training cohort. These sequential variants extend fregression to right-censored settings while preserving its generative flexibility.

5.2 Estimation

The population version of estimation formula for g_c is similar to (7), with the response C_i replaced by (Z_i, X_i) . Estimation objectives of g, f, h are the same as in (7) and (8) respectively, only now the outcome variable contains T time steps of dimension $d_y \times T$, and here we specify causal estimand of interest to be conditional on baseline covariates, which can be customized according to the specific question of interest. More formally, the population solution to φ_s can be expressed as:

$$\begin{aligned} g_c^* &:= \underset{g_c}{\operatorname{argmin}} \mathbb{E} \left[\|C - g_c(\epsilon_c)\| - \frac{1}{2} \|g_c(\epsilon_c) - g_c(\epsilon'_c)\| \right] \\ g^* &:= (g_0^*, \dots, g_{T-1}^*) = \underset{g}{\operatorname{argmin}} \mathbb{E} \left[\|(Z, X) - g(\epsilon)\| - \frac{1}{2} \|g(\epsilon) - g(\epsilon')\| \right] \\ (f^*, h^*) &:= (f_0^*, \dots, f_{T-1}^*, h_0^*, \dots, h_{T-1}^*) \\ &= \underset{f, h}{\operatorname{argmin}} \mathbb{E} \left[\|Y - f(C, X, \tilde{\eta})\| - \frac{1}{2} \|f(C, X, \tilde{\eta}) - f(C, X, \tilde{\eta}')\| \right] + \mathbb{E} \left[\|\eta - \bar{\eta}\| - \frac{1}{2} \|\bar{\eta} - \bar{\eta}'\| \right] \end{aligned}$$

where $\epsilon_c, \epsilon'_c \stackrel{\text{i.i.d.}}{\sim} \mathcal{N}(0, I_{d_c})$; $\epsilon, \epsilon' \stackrel{\text{i.i.d.}}{\sim} \mathcal{N}(0, I_{(d_z+d_x) \times T})$; $\tilde{\eta} = h(Z, X, \xi)$, $\tilde{\eta}' = h(C, Z, X, \xi')$, $\bar{\eta} = h(C, \bar{Z}, \bar{X}, \xi'')$, and $\bar{\eta}' = h(\bar{Z}', \bar{X}, \xi''')$ with $\eta \sim \mathcal{N}(0, I_{d_y \times T})$, $\xi, \xi', \xi'', \xi''' \stackrel{\text{i.i.d.}}{\sim} \mathcal{N}(0, I_{d_y \times T})$, $(Z, X) \sim \mathbb{P}_{ZX|C}$, $\bar{X} \sim \mathbb{P}_X$ and $\bar{Z}, \bar{Z}' \stackrel{\text{i.i.d.}}{\sim} \mathbb{P}_{Z|C\bar{X}_{T-2}}$. Similar to that in the static setting, we learn auxiliary models $e := (e_0, e_1, \dots, e_{T-1})$ to match $\mathbb{P}_{Z|C\bar{X}_{T-2}}$ via standard engression models at each time step t :

$$\begin{aligned} e_0^* &:= \underset{e_0}{\operatorname{argmin}} \mathbb{E} \left[\|Z_0 - e_0(C, \zeta_0)\| - \frac{1}{2} \|e_0(C, \zeta_0) - e_t(C, \zeta'_0)\| \right] \\ \text{and } e_t^* &:= \underset{e_t}{\operatorname{argmin}} \mathbb{E} \left[\|Z_t - e_t(C, \bar{X}_{t-1}, \zeta_t)\| - \frac{1}{2} \|e_t(C, \bar{X}_{t-1}, \zeta_t) - e_t(C, \bar{X}_{t-1}, \zeta'_t)\| \right], \end{aligned}$$

where $\zeta_0, \zeta'_0, \zeta_t, \zeta'_t \stackrel{\text{i.i.d.}}{\sim} \mathcal{N}(0, I_{d_z})$, for $t \in \{1, \dots, T-1\}$.

Because treatments vary over time, we impose the standard *sequential conditional exchangeability* assumption to ensure identification. For detailed discussions, see Hernán and Robins (2025) and Evans and Didelez (2024, Remark 1.5; Sections 6–7).

Corollary 5.1 (Sequential model preserves correctness). *If at each time point the static fregression model satisfies the correctness property (Proposition 2.2), then the joint sequential model also satisfies correctness.*

Corollary 5.2 (Sequential model preserves consistency). *If at each time point the static fregression model enjoys consistency (Theorem 3.1), then the joint sequential model is likewise consistent.*

Corollary 5.3 (Sequential model preserves extrapolation). *If at each time point the static fregression model allows extrapolation on continuous treatments (Proposition 4.1), then the joint sequential model also admits extrapolation on continuous treatments at every time point.*

Proof of Corollaries 5.1–5.3. The proof proceeds by the induction on t . For the base case $t = 0$, the claims reduce to the static fregression result. Now suppose the statement is true for all time steps up to $t - 1$. Applying the static result to φ_t establishes the properties for time t . \square

5.3 Sampling

The sampling works similarly to the static fregression with sequential chaining. Similar to Section 2.5, we provide sampling from φ_s^* for the following scenarios.

1. Simulate \widehat{C} : Draw $\varsigma \sim \mathcal{N}(0, I_{d_c})$ and apply the transformation $g_c^*(\varsigma)$.
2. Simulate $(\widehat{Z}, \widehat{X}) \in \mathbb{R}^{T \times (d_z + d_x)}$: Specify c (can be simulated from $g_c^*(\varsigma)$) and sample $\epsilon_0 \sim \mathcal{N}(0, I_{d_z + d_x})$; apply $g_0^*(\cdot)$ on (c, ϵ_0) to get $(\widehat{Z}_0, \widehat{X}_0)$. Then, for $t = 1, \dots, T - 1$: simulate $\epsilon_t \sim \mathcal{N}(0, I_{d_z + d_x})$, then $(\widehat{Z}_t, \widehat{X}_t) = g_t^*(c, \widehat{Z}_{t-1}, \widehat{X}_{t-1}, \epsilon_t)$. Putting them together we obtain $(\widehat{Z}, \widehat{X}) \in \mathbb{R}^{T \times (d_z + d_x)}$.
3. Simulate $\widehat{Y}(\bar{x}_{T-1})$: For $t = 1, \dots, T - 1$, sample $\eta_t \sim \mathcal{N}(0, I_{d_y})$, then apply the transformation f_t^* with sampled η_t and specified \bar{x}_t to get $\widehat{Y}_t = f_t^*(\bar{x}_t, \eta_t)$. Putting them together, we obtain $\widehat{Y} = (\widehat{Y}_0, \dots, \widehat{Y}_{T-1})$.
4. Simulate from φ_s to obtain $(\widehat{C}, \widehat{Z}_t, \widehat{X}_t, \widehat{Y}_t) \in \mathbb{R}^{d_c + T \times (d_z + d_x + d_y)}$: follow the instructions above to obtain \widehat{C} , \widehat{Z}_t , \widehat{X}_t . For $t = 0, \dots, T - 1$, sample $\xi_t \sim \mathcal{N}(0, I_{d_y})$, and apply the transformation h_t^* on sampled $(\widehat{C}, \widehat{Z}_t, \widehat{X}_t, \xi_t)$ to get $\tilde{\eta}_t = h_t^*(\widehat{C}, \widehat{Z}_t, \widehat{X}_t, \xi_t)$. We obtain \widehat{Y}_t via $\widehat{Y}_t = f_t^*(\widehat{X}_t, \tilde{\eta}_t)$.

Proposition 5.1 (Simulate data from joint distribution). *We take sequential conditional exchangeability and that Assumption 2.1 holds. The simulation procedure stated above generates a draw \mathbb{P}_φ of (C, Z, X, Y) whose law equals the observed joint distribution of (C, Z, X, Y) .*

Proof. We proceed by induction on the time index t . For $t = 0$, first sample $\widehat{C} \sim \mathbb{P}_{g_c}$. Conditional on \widehat{C} , draw $(\widehat{Z}_0, \widehat{X}_0) \sim \mathbb{P}_{Z_0 X_0 | C = \widehat{C}}$ by applying $g_0^*(\cdot)$ on $(\widehat{C}, \epsilon_0)$, where $\epsilon_0 \sim \mathcal{N}(0, I_{d_z + d_x})$. Draw $\xi_0 \sim \mathcal{N}(0, I_{d_y})$, then apply h_0^* on sampled $\widehat{C}, \widehat{Z}_0, \widehat{X}_0, \xi_0$ to get $\tilde{\eta}_0$. Obtain \widehat{Y}_0 by applying $f_0^*(\cdot)$ on $(\widehat{X}_0, \tilde{\eta}_0)$. Guaranteed by Proposition 2.2, $(\widehat{Z}_0, \widehat{X}_0) \sim \mathbb{P}_{Z_0 X_0 | C = \widehat{C}}$, $\widehat{Y}_0 \sim \mathbb{P}_{Y_0 | C = \widehat{C}, Z_0 = \widehat{Z}_0, X_0 = \widehat{X}_0}$. This takes care of the base case.

Suppose that for $t \geq 1$, $(\widehat{C}, \widehat{Z}_{t-1}, \widehat{X}_{t-1}, \widehat{Y}_{t-1}) \sim (C, \overline{Z}_{t-1}, \overline{X}_{t-1}, \overline{Y}_{t-1})$. We now extend to time t by drawing $(\widehat{Z}_t, \widehat{X}_t)$ from the distribution of $(Z_t, X_t \mid C = \widehat{C}, \overline{Z}_{t-1} = \widehat{Z}_{t-1}, \overline{X}_{t-1} = \widehat{X}_{t-1})$ and then \widehat{Y}_t is sampled from $Y_t \mid C = \widehat{C}, \overline{Z}_t = \widehat{Z}_t, \overline{X}_t = \widehat{X}_t$, using the procedure stated in the above simulation settings. Applying the chain rule yields $(\widehat{C}, \widehat{Z}_t, \widehat{X}_t, \widehat{Y}_t) \sim (C, \overline{Z}_t, \overline{X}_t, \overline{Y}_t)$, which completes the inductive step. \square

6 Numerical Examples on Supported Settings

In this section, we evaluate fregression on synthetic benchmarks under both static and time-varying treatment regimes. Our evaluation focuses on two key aspects:

1. *Estimation and inference.* We evaluate how precisely fregression recovers the underlying data-generating process, especially the marginal interventional quantities. To establish ground truth, we either use existing datasets or simulate new ones with known interventional distributions, employing two packages built on frugal parameterization: the `causl` package (Evans, 2021a) for static treatment settings, and the `surviv1` package (Evans, 2021b) for longitudinal and survival data. Simulating data this way gives us exact control over the marginal quantity targets.
2. *Simulation performance.* We assess fregression’s ability to sample new data that both preserves the original data’s properties and matches the specified marginal interventional distributions. By comparing the generated samples with the original targets, we verify that our model can capture and replicate complex distributional patterns.

In the experiments that follow, we compare fregression against leading, specialized methods in each domain. While these competitors excel in their specific settings, none combine the estimation and simulation on static treatments, longitudinal dynamics, survival outcomes, and continuous treatments in a single framework. This breadth underscores fregression’s unique, comprehensive applicability. The code for reproducibility can be found at <https://github.com/xwshen51/fregression>.

6.1 Binary Intervention

Estimating a treatment effect under a binary intervention via fregression does not require propensity score estimation or adjustment; instead, it directly models the marginal interventional quantity of interest. This contrasts with methods that average outcome-regression predictions over the covariate distribution, whose performance can suffer when certain covariate combinations are rare or poorly represented. By focusing on the marginal causal parameter, fregression avoids the instability caused by extreme propensity score values. We assess its robustness under weak overlap scenarios, especially in finite samples, to demonstrate its ability to recover causal effects even when classical overlap conditions are violated. We first investigate how fregression handles weak overlap using synthetic data.

We simulate $p = 10$ baseline covariates $Z = (I, C)$, where the instrumental variables $I \in \mathbb{R}^5$ and the confounders $C \in \mathbb{R}^5$ are generated independently as standard normals. Treatment assignment follows $X \mid Z \sim \text{Bernoulli}(\pi(Z))$ with $\pi(Z) = \text{logit}(\beta_I^\top I + \mathbf{1}^\top C)$, $\beta_I \in \mathbb{R}^5$ and the outcome is $Y(x) \sim \mathcal{N}(2x, 1)$, with Gaussian copulae between each confounders $C_j, j \in 1, \dots, 5$ and Y with correlation $\rho = 2\text{logit}(1) - 1 \approx 0.46$. By increasing the magnitude of the instrumental coefficients β_I , we push the propensity scores toward 0 or 1, creating a weak-overlap scenario.

For each iteration, we simulate $N = 5000$ observations and repeat the experiment for $K = 30$ iterations. Let $\hat{\theta}_k$ be the ATE estimate in the k th iteration and θ the true ATE. We report bias, mean absolute error (MAE), and root mean squared error (RMSE). We compare fregression against the augmented inverse probability weighted (AIPW) estimator (with logistic regression to estimate propensity score and Random Forests as the outcome regression model), Dragonnet, and CausalEGM. TARNet, CFRNet and CEVAE demonstrated sensitivity to hyperparameters and performed poorly, hence we exclude these results. Furthermore, these methods were primarily proposed for conditional treatment effect quantities, rather than marginal causal effects.

Results in Table 2 show that the AIPW estimator's variance increases as overlap worsens, while fregression remains stable. Even without per-dataset hyperparameter tuning, fregression matches or outperforms Dragonnet and CausalEGM in bias, MAE, and RMSE across all regimes. We present the experiment details in Appendix C.1.

β_I		Fregression	AIPW	CausalEGM	Dragonnet
	metric				
0.0	RMSE	0.056	0.290	0.151	0.070
	Bias	-0.000	0.225	-0.117	0.031
	MAE	0.048	0.253	0.130	0.056
0.5	RMSE	0.076	0.290	0.149	0.114
	Bias	-0.019	0.258	-0.124	0.042
	MAE	0.059	0.258	0.132	0.100
1.0	RMSE	0.071	0.849	0.193	0.055
	Bias	-0.015	0.480	-0.173	0.015
	MAE	0.056	0.480	0.173	0.039
1.5	RMSE	0.086	0.690	0.262	0.155
	Bias	-0.028	0.530	-0.245	0.080
	MAE	0.069	0.543	0.245	0.117
2.0	RMSE	0.084	0.524	0.287	0.113
	Bias	-0.026	0.437	-0.274	0.028
	MAE	0.071	0.466	0.274	0.095

Table 2: Estimation performance across different degrees of overlap.

Twins		Hirano & Imbens	Sun
p	50	200	200
Z	Real data derived from all births in the USA between 1989–1991.	$(Z_1, \dots, Z_p) \stackrel{\text{i.i.d.}}{\sim} \text{Exp}(1)$	$(Z_1, \dots, Z_p) \stackrel{\text{i.i.d.}}{\sim} \mathcal{N}(0, 1)$
$Y(x) Z$	$Y = 1: \text{death.}$ $Y(x) \sim \text{Bernoulli}(R(x)),$ $R(x) = -\frac{2}{1 + e^{-3x}} + z^\top \gamma + \epsilon,$ $\gamma_i \sim \mathcal{N}(0, 0.025^2), \epsilon \sim \mathcal{N}(0, 0.25^2)$	$\mathcal{N}(x + (Z_0 + Z_2)e^{-x(Z_0 + Z_2)}, 1)$	$\mathcal{N}(x + Z_1 + \cos(Z_2) + Z_5^2 + Z_6 - \frac{1}{2}, 1)$
$X Z$	weights (observed)	$\exp(Z_0 + Z_1)$	$\mathcal{N}(-2 \sin(2Z_1) + Z_2^2 + Z_3 + \cos(Z_4) - \frac{5}{6}, 1)$
$\mu(x)$	$-\frac{2}{1 + e^{-3x}} + \mathbb{E}[Z^\top \gamma]$	$x + \frac{2}{(1+x)^3}$	$x + 0.5 + e^{-0.5}$

Table 3: Key information of the three datasets in continuous treatments, including the dimension of covariates p , the data generation process of Z, X, Y and the ground truth ADRF $\mu(x)$.

ADRF Estimates

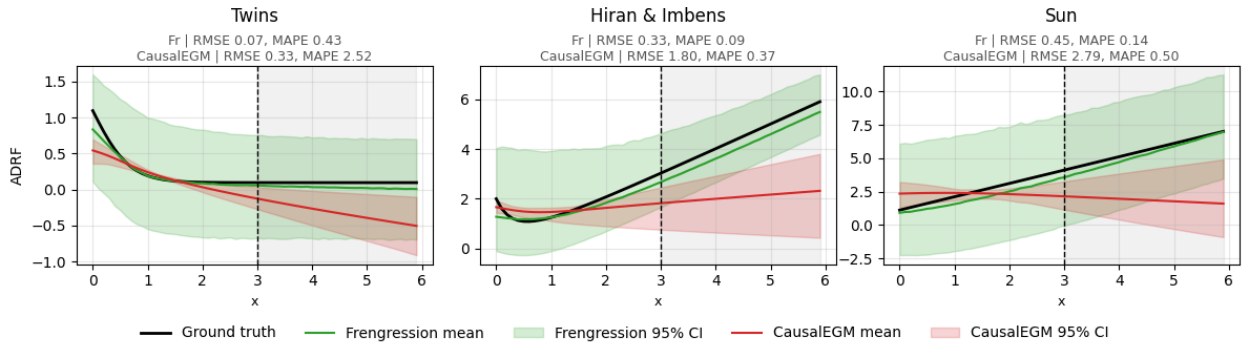


Figure 4: ADRF estimation, with RMSE and MAPE, fregression (Fr) and CausalEGM, across 30 simulations. We sample 1000 datapoints for training for each dataset. The grey area is not seen during training. We train both models for 1000 epochs in all simulations.

6.2 Continuous Treatment

In the context of continuous treatment, obtaining the average dose-response function (ADRF), defined as $\mu(x) = \mathbb{E}_Z[Y(x) | Z]$, is typically of interest. To evaluate the models' performance, we use RMSE and mean absolute percentage error (MAPE).

We follow Liu et al. (2024) in the synthetic experiments for continuous treatment, using the same data: two synthetic datasets, Hirano and Imbens (2004) and Sun et al. (2015); and one semi-synthetic dataset, Twins, containing weights, mortality and other covariates of all 71,345 pairs of twins born in the USA between 1989–1991. For the two synthetic datasets, we trained the models on 1000 samples. The detailed information can be found in the supplementary appendix of Liu et al. (2024). We present the key information in Table 3.

Figure 4 compares ADRF estimates from fregression and CausalEGM on the three benchmark datasets over $K = 30$ simulations. We trained both models for 1000 epochs in all experiments. For

CausalEGM specifically, we used the best model configuration provided by their package.

For each simulation k and treatment level x , we compute the average of 1000 draws from the learned fregression model as the estimated treatment effect on level x . We then aggregate across simulations to obtain the ensemble estimate $\hat{\mu}(x) = \frac{1}{K} \sum_{k=1}^K \hat{\mu}^k(x)$, plotted as a solid green line for fregression and a red line for CausalEGM.

To illustrate uncertainty, we add shaded bands corresponding to the 2.5%–97.5% interval. For the k th simulation of fregression, let $\hat{q}_\alpha^k(x)$ be the empirical α quantiles of the 1000 samples from $\hat{\mathbb{P}}_{Y(x)}^{*,k}$. The band at x is then

$$\left[\frac{1}{K} \sum_{k=1}^K \hat{q}_{2.5\%}^k(x), \frac{1}{K} \sum_{k=1}^K \hat{q}_{97.5\%}^k(x) \right].$$

Since CausalEGM produces point estimates only, we take the 2.5% and 97.5% sample quantiles of $\{\hat{\mu}^k(x)\}_{k=1}^K$ to form its shaded band.

We assessed each model’s ability to recover the dose-response function on a treatment range unseen during training by withholding treatments in the interval $(3, 6]$ from the fitting process. After training, we estimated the ADRF over the full treatment range, including the held-out region $x \in (3, 6]$, and compared the estimated ADRF the ground truth. As shown in Figure 4, fregression consistently outperformed CausalEGM across all three benchmark datasets, showing superior accuracy both within the training range and in the extrapolation interval, and did so without any additional hyperparameter tuning. The estimated 2.5% and 97.5% quantile bands accurately bound the true ADRF across all treatment levels.

6.3 Longitudinal Setting & Survival Data

We demonstrate the modelling on longitudinal data. To the best of our knowledge, only a few deep learning framework have been proposed regarding inference and simulation on marginal causal effects. The recent work Shirakawa et al. (2024) that combines the Transformer architecture and LTMLE, handles only estimation of causal effects on binary treatment in the longitudinal context.

We designed four synthetic settings to showcase the flexibility of fregression. Settings 1–3 are designed for survival analysis, and setting 4 is longitudinal. In settings 1–3, we denote \tilde{Y}_t as the residual lifetime after surviving to time t . If $\tilde{Y}_t < 1$, then $Y_t = 1$, otherwise $Y_t = 0$. The details of each setting are given below in Appendix C.2.1. We provide the summary of key information as below:

- Setting 1: $T = 10$. C is drawn from a Bernoulli distribution. We set the treatment X_t to be binary and dependent on (Z_t, C) ; the time-varying covariate Z_t is dependent on previous treatment X_{t-1} and C ; the outcome $\tilde{Y}(\bar{x}_t) \mid C$ follows an exponential distribution.
- Setting 2: $T = 10$. C is drawn from an exponential distribution with rate 1 and Z_0 from a standard normal; $X_0 \mid Z_0 \sim \text{Bernoulli}(\text{logit}(-0.5 + 0.5Z_0))$; the treatment X_t is still binary, and is dependent on both Z_t and the previous treatment X_{t-1} ; the time-varying covariate Z_t

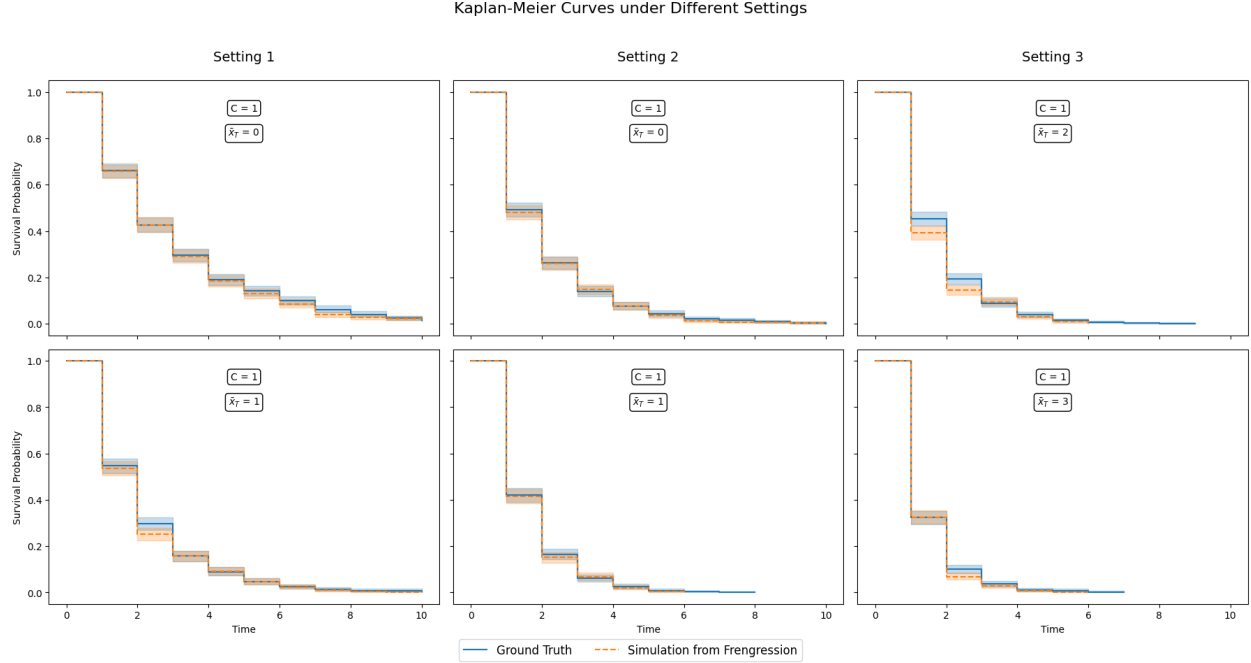


Figure 5: Kaplan-Meier curves of data generated from true data generating process and simulated from fitted fregression.

depends on X_{t-1} , C and Z_{t-1} . The Spearman correlation between Y_t and Z_{t-1} is 0.2, and that for Y_t and Z_t given Z_{t-1} is 0.3. Compared to setting 1, setting 2 has more complicated dependency.

- Setting 3: $T = 10$. C is drawn from a Bernoulli distribution. We set X_t to be continuous from a normal distribution, dependent on Z_{t-1} and C . We use a Gaussian copula with correlation 0.4 between Z_t and Y_t . In this setting the treatment is continuous.
- Setting 4: $T = 5$. C is drawn from a standard normal distribution. We set X_t to be continuous from normal distribution, and the outcome $Y_t(\bar{x}_t) | C \sim \mathcal{N}(2x_t + x_{t-1} + 0.5x_{t-2} + C, 1)$. This models the longitudinal scenario: at time step t we are able to observe a continuous outcome rather than just the indicator of event occurrence.

In each setting, we simulate $n = 6000$ samples for training. We then sample 1000 datapoints from each fitted model. In Figure 5, we compare Kaplan-Meier curves fitted on the true data-generating process with those simulated by fregression with intervention x_t fixed the same across time. Note that fregression is trained on time-varying covariates and interventions as described above. This supports our claim on the flexibility and comprehensiveness of the fregression model.

To create a performance baseline, we also fit Deep LTMLE using the `dltmle` package (Shirakawa, 2024) to setting 1. Our causal estimand is the risk difference between always-treated and always-placebo regimens over the entire follow-up horizon $\theta = \mathbb{E} Y_{T-1}(\mathbf{1}) - \mathbb{E} Y_{T-1}(\mathbf{0})$, where as before, $Y_t = 1$ if the event occurs during time zone $(t-1, t]$ and 0 otherwise. If we set $T = 5$, the true value of θ is 0.11. Over 10 simulation runs, Deep LTMLE's mean estimate was 0.13 (SD 0.03),

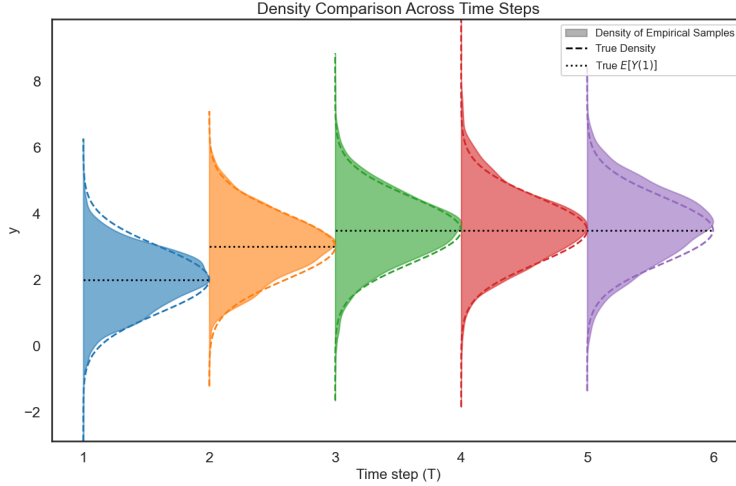


Figure 6: Density comparison of data simulated from fregression vs. true density, Setting 4.

and fregression’s was 0.09 (SD 0.04). These results are similar, and fregression achieves them without a separate targeting step for calibration with explicit form of influence function needed, thus it can be applied to a broader class of causal estimands. We would also like to highlight the computational efficiency of fregression compared to `dltmle`. Hyperparameter tuning with `dltmle`’s default `Optuna` routine took about 30 minutes for 10 trials, plus 4 minutes to run 100 training epochs, whereas fregression completed 2000 epochs in 1.4 minutes on the same hardware.

Figure 6 shows the results for Setting 4, where we plot the density of 5000 points simulated from the interventional distribution $\hat{\mathbb{P}}_{Y(x)|C}$ estimated by fregression and set $x = \mathbf{1}$, $C = 0$. As expected, the fregression fit closely matches the true interventional distribution, although the performance worsens slightly at the last time step $T = 5$ due to growing complexity.

6.4 Distributional Regression

In practical applications, it is often necessary to simulate data under a pre-specified interventional distribution while preserving the empirical dependencies observed in the original sample. As a distributional-regression framework, fregression can estimate the target marginal interventional law of the observed data; it also allows one to generate synthetic datasets that retain the observed correlation structure between the covariates and treatments, but target an arbitrarily specified marginal causal distribution.

In Figure 7, we illustrate our method in the RCT (no confounding variables) context by comparing the empirical histogram from fregression’s simulations with the ground truth, and showcase its ability to simulate data with user-specified marginal causal distributions while preserving the joint dependency structure of the covariates and treatment.

First, we generate $n = 5000$ samples from the true data-generating process: the six covariates $Z \in \mathbb{R}^6$ are independently drawn from $\mathcal{N}(0, 1)$, the treatment $X \sim \text{Bernoulli}(0.5)$ as commonly seen

Top: Simulated $Y|X$ | Middle: True $Y(x)$ | Bottom: Correlations on Simulated Data

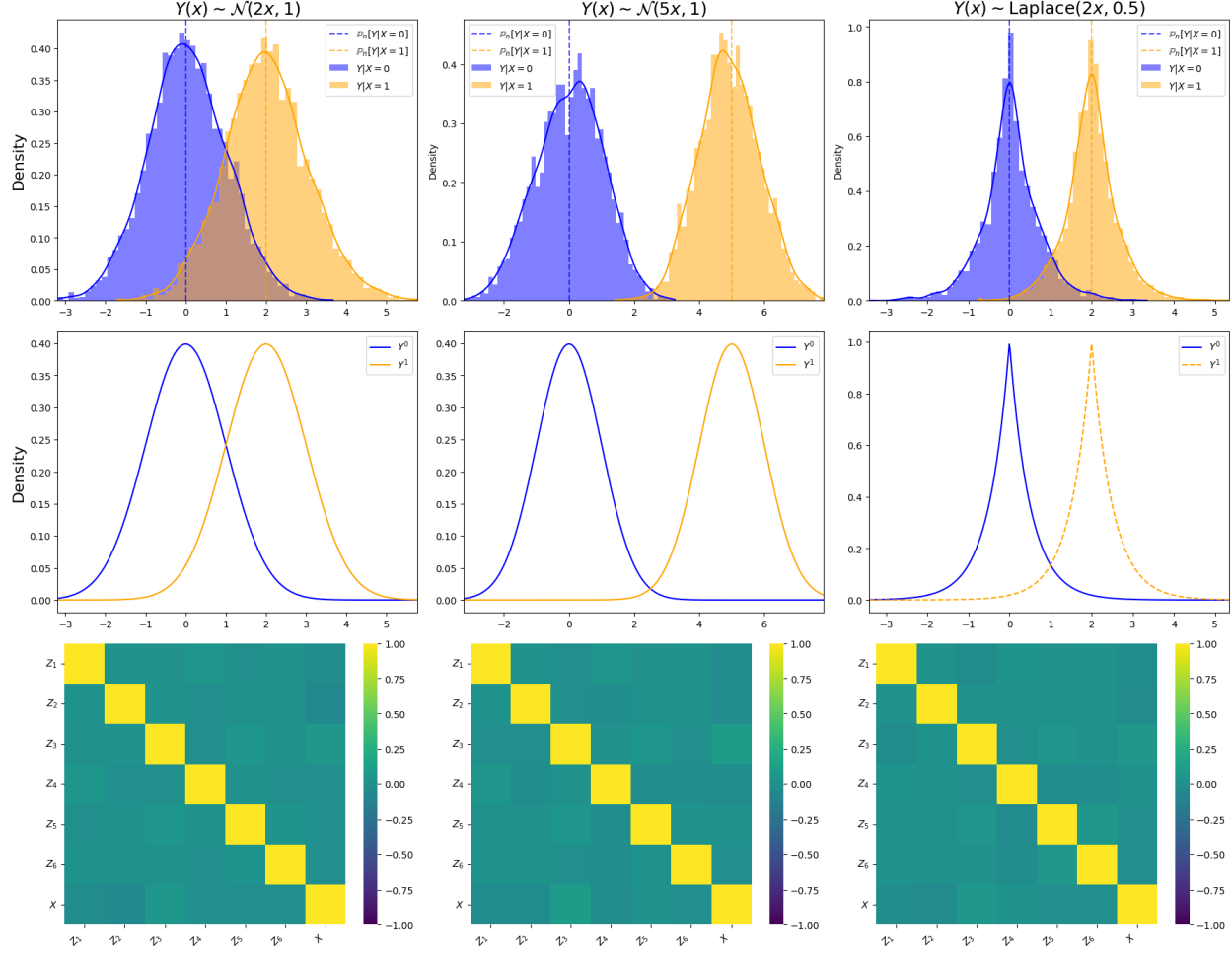


Figure 7: Marginal densities of simulations from fregression (top row), target (middle row) and correlation of covariates and treatment on simulations from fregression (bottom row).

in an RCT, and the intervened outcome $Y(x) \sim N(2x, 1)$, with a Gaussian copula between Z_5, Z_6 to Y with Pearson correlation $\rho = 2 \text{expit}(1) - 1 \approx 0.46$. Fitting fregression to these samples recovers the true interventional distribution and the correlation between X and Z (left column).

Next, we replace the fitted $Y(x)$ marginal with two new targets: $N(5x, 1)$ and Laplace($2x, 0.5$), and draw $n = 5000$ simulated triples $(\widehat{Z}, \widehat{X}, \widehat{Y})$ from the modified model (middle and right columns). In Figure 7, the top row shows the estimated marginal densities of $Y|X=0$ and $Y|X=1$ from the simulated data. Because there is no confounding, these curves should match the true interventional marginals. The middle row displays the true target densities (the Gaussians or Laplace) for each intervention; we see that the simulation from the fregression fits align with these densities. The bottom row confirms that the original joint distribution of (Z, X) remains unchanged under the modified interventional model. The results validate that in all cases, the simulated marginals match the newly specified objectives while preserving the baseline dependencies between X and Z .

7 Application on LEADER

We illustrate fregression on the LEADER trial (Novo Nordisk A/S, 2015) to showcase its ability to simulate realistic, time-to-event data with complex covariate patterns. LEADER is a randomized, double-blind, placebo-controlled cardiovascular outcomes trial that enrolled 9340 patients with type 2 diabetes at high cardiovascular risk, randomizing patients into liraglutide (up to 1.8 mg daily) or placebo, both on top of standard care, resulting in equal sizes of the two arms. Patients were recruited from August 2010 through April and followed for 3.5–5 years, with a median follow-up of 3.8 years. The primary endpoint is time to first major adverse cardiovascular event (MACE), including cardiovascular death, non-fatal myocardial infarction and non-fatal stroke. The original analysis found that MACE occurred in significantly fewer patients in the liraglutide group than in the placebo group (Marso et al., 2016).

To build our generative model, we select baseline covariates known to predict MACE. The baseline covariates include four binary indicators: gender, smoker status, carotid stenosis $> 50\%$ on angiography, and diabetic nephropathy at screening. We have seven continuous variables at baseline: age, duration of diabetes (months), high-density lipoprotein (HDL) cholesterol, low-density lipoprotein (LDL) cholesterol, total cholesterol, triglycerides, and serum creatinine. We also incorporated three key time-varying biomarkers to capture longitudinal risk dynamics: HbA1c, body-mass index (BMI), and estimated glomerular filtration rate (eGFR). The description of the variables can be found in Table 9.

We partition the trial timeline into 6-month intervals over a maximum of 60 months, yielding 11 discrete timepoints (i.e. $t = 0, 1, 2, \dots, 10$). We define each subject’s event time as $k \in (0, \infty)$, where $k \in (0, 10]$ indicates the time MACE occurred in units of 6-month intervals, and $k > 10$ indicates no event within the trial. With this notation, we define the event indicators Y_t , $t \in \{0, 1, \dots, 10\}$ as

$$Y_t = \begin{cases} 1, & k \leq t, \\ 0, & \text{otherwise.} \end{cases}$$

Here, we have $Y_t = 1$ if and only if the event occurred before t , otherwise $Y_t = 0$.

Note that in the time-varying setting, covariates were recorded at different intervals: HbA1c was measured every 6 months, whereas BMI and eGFR were collected only at months 6, 12, 18, 30, 48, and 60 from the start of the trial. To retain as much information as possible, we impute missing BMI and eGFR values at intermediate timepoints using the most recent available measurement (last observation carried forward).

We exclude units missing any baseline covariates, leaving 9161 subjects. We take the logarithm of triglycerides and serum creatinine. We then normalize all continuous covariates by subtracting their mean values and dividing them by their standard deviations. After fitting fregression to the processed dataset, we simulate 9161 synthetic records from the model for 5000 times.

Figures 8–10 visualize fregression’s empirical performance on data simulation. For each variable at each time point, we compute the RMSE between the mean of the simulated samples and the true mean. Overall, fregression accurately reproduces the linear correlations and achieves low RMSE across both baseline and time-varying covariates. However, as shown in Figure 8,

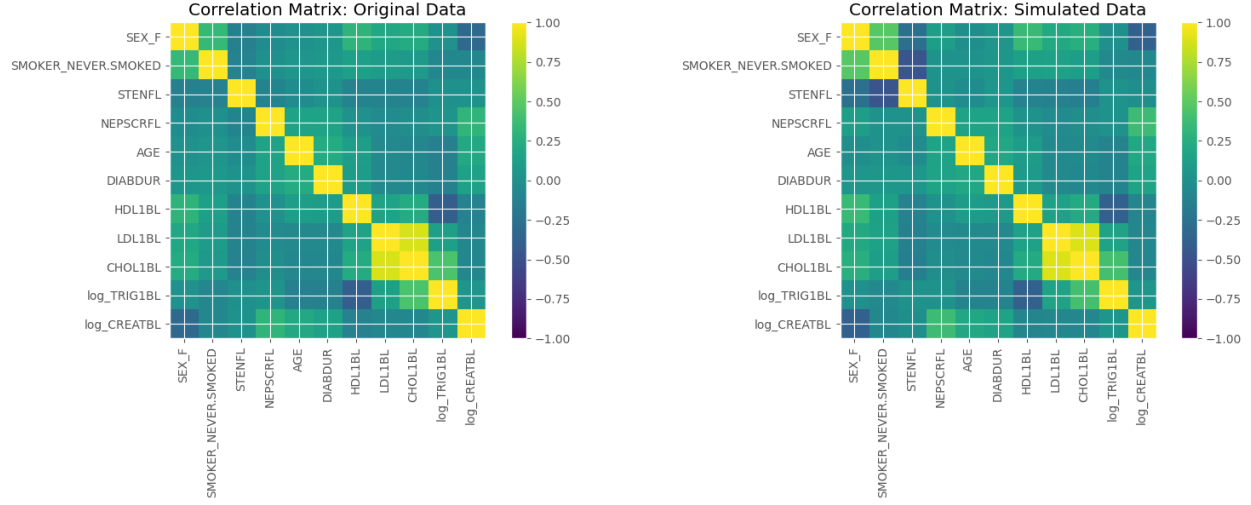


Figure 8: Correlation matrix of baseline covariates, real data vs. data simulated from fitted frengression. The heatmap illustrates the similarity of simulated data with real data regarding correlation coefficient.

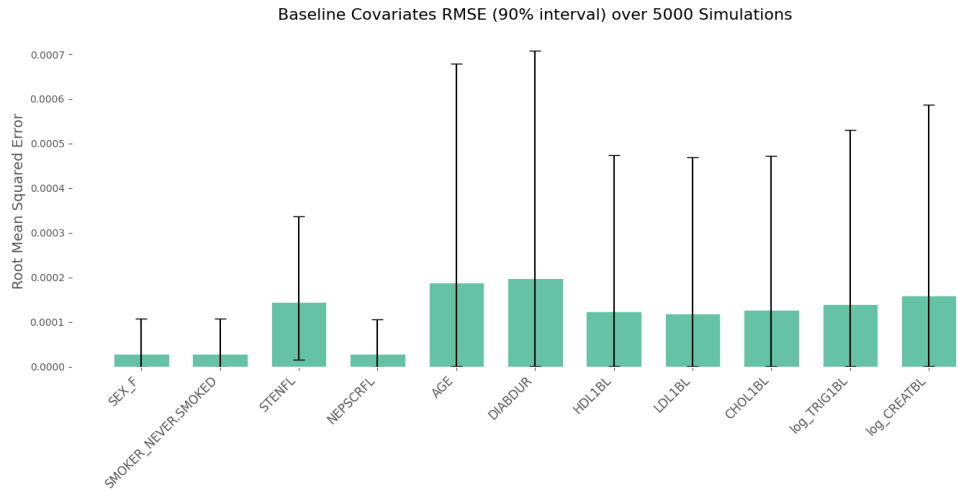


Figure 9: RMSE of each baseline covariate (continuous variables are normalized), with the maximum RMSE less than 0.001 over 5000 simulations.

the simulated correlations of the STENFL variable (carotid $> 50\%$ stenosis on angiography) with SEX_F (gender) and SMOKER_NEVER.SMOKE (indicating smoking status) deviate from that of the true data, reflecting the greater challenge of modelling binary variables using deep generative models compared to continuous ones.

To quantify how well the simulated data match the originals, we train logistic classifiers to distinguish real observations from simulated ones. On baseline covariates, the mean AUC is 0.50 (range 0.47–0.52), indicating classification that is nearly random. For the joint datasets (including baseline covariates, time-varying covariates and MACE occurrence), the mean AUC is 0.55 (range 0.52–0.57), still reflecting substantial similarity between simulated and real distributions.

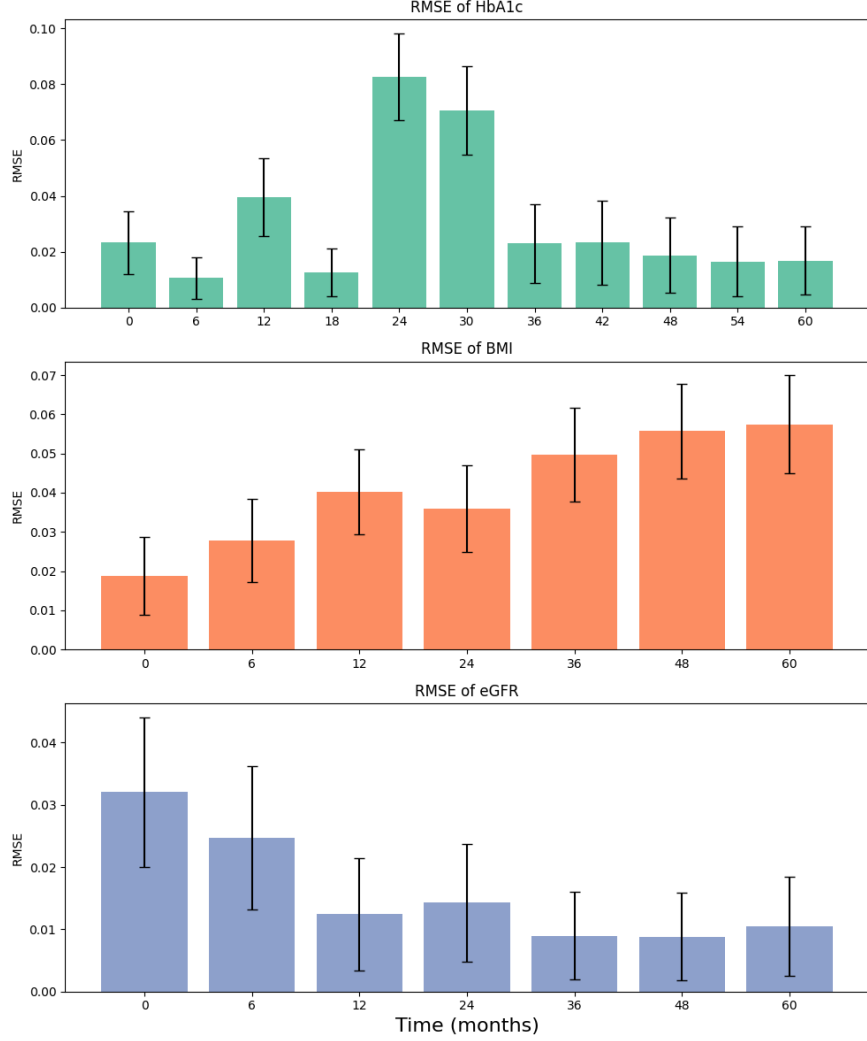


Figure 10: RMSE of each time varying covariate (normalized) across different time-points over 5000 simulations. All of them are of small scales (maximum 0.1).

We also sample event occurrences from the fitted interventional distribution $\hat{\mathbb{P}}_{Y(x)|C}$. Over 5000 simulations, the mean MACE occurrence rate in the placebo arm is 14.7% with 90% interval [13.8%, 15.6%] (5th and 95th quantiles of the 5000 estimates), and in the liraglutide arm it is 13.0% with 90% interval [12.2%, 13.9%]. These values align exactly with the 14.7% in the placebo arm and 13.0% in the liraglutide arm from real data, confirming that fregression faithfully captures both covariate structures and event frequencies.

8 Discussion

The rapid growth of AI makes reliable causal inference more important than ever. Contributing to this, we introduce a deep generative approach that generates synthetic data meeting specified marginal interventional distribution, while maintaining a realistic level of complexity. Such a data

generation tool is helpful in different applications, including pre-experiment study design for randomized controlled trials, selecting an inference procedure, and stress testing AI methods (Giuffrè and Shung, 2023; Pezoulas et al., 2024).

There are several promising extensions. As noted in Remark 2.2, the variation independent decomposition in fregression can be directly adapted for differentially private simulation. Although differential privacy remains the gold standard for protecting individual records, its strict requirements often come at the expense of simulation accuracy in practice. This means that suitable measures require a better understanding of the needs of end users (Yoon et al., 2020; Kenny et al., 2021; McCartan et al., 2023).

Methodologically, although fregression can generate data of subject-level trajectories under time-varying treatment, or any quantity conditional on a subset of covariates, its robustness and efficiency for individual treatment effects, such as those needed for dynamic treatment regimes, remain open questions. Even so, we find that centring on the target causal distribution explicitly brings clarity and consistency in both estimation and simulation.

At present, fregression’s extrapolation works only with continuous treatments; how best to extrapolate when treatments are discrete is to be explored. In addition, we provided consistency results for the generative model. Deriving convergence rates would help us build valid confidence intervals for the estimates that fregression produces.

Acknowledgments

We thank Jens Magelund Tarp for helping with the analysis on the LEADER trial and advice on applications. Linying Yang is supported by the EPSRC Centre for Doctoral Training in Modern Statistics and Statistical Machine Learning (EP/S023151/1) and Novartis. Robin J. Evans is supported by GSK. We acknowledge funding administered by the Danish National Research Foundation in support of the Pioneer Centre for SMARTbiomed.

A Main proofs

A.1 Proof of Proposition 2.1

Proof. When the conditions in Assumption 2.2 hold, we have

$$p_{Y(x)}(y) = p_{Y(x)|X_0}(y | x_0) \quad (13)$$

$$= p_{Y(X_0, x_1)|X_0}(y | x_0) \quad (14)$$

$$= \int_{\mathcal{Z}} p_{Y(X_0, x_1)|X_0Z}(y | x_0, z) p_{Z|X_0}(z | x_0) dz \quad (15)$$

$$= \int_{\mathcal{Z}} p_{Y(X_0, x_1)|X_0ZX_1}(y | x_0, z, x_1) p_{Z|X_0}(z | x_0) dz \quad (16)$$

$$= \int_{\mathcal{Z}} p_{Y|X_0ZX_1}(y | x_0, z, x_1) p_{Z|X_0}(z | x_0) dz, \quad (17)$$

where (13) and (16) are from the unconfoundedness assumption, while (14) and (17) are based on the consistency assumption. Equation (15) is from the law of total probability; (13), (15) and (16) require the positivity assumption. \square

A.2 Proof of Proposition 2.2

Proof. Since the energy score is a strictly proper scoring rule (Gneiting and Raftery, 2007), the objective function in (7) is minimized if and only if $g(\epsilon) \sim \mathbb{P}_{ZX}$. By Assumption 2.1, such a model exists, we hence have $g^*(\epsilon) \sim \mathbb{P}_{ZX}$. According to Proposition 1 of Shen and Meinshausen (2024) and Assumption 2.1, we have $f^*(x, h^*(z, x, \xi)) \sim \mathbb{P}_{Y|Z=z, X=x}$. Similarly, the second term of (8) is minimized if

$$h^*(Z, x, \xi) \sim \mathcal{N}(0, I_{d_y}) \text{ when } Z \sim \mathbb{P}_{Z(x)}, \quad (18)$$

for all $x \in \mathcal{X}$.

The identification formula in Proposition 2.1,

$$p_{Y(x)}(y) = \int_{\mathcal{Z}} p_{Y|X_0ZX_1}(y | x_0, z, x_1) p_{Z|X_0}(z | x_0) dz.$$

suggests that to sample from $\mathbb{P}_{Y(x)}$ for any given $x = (x_0, x_1) \in \mathcal{X}$, we can

- (i) first sample Z from $\mathbb{P}_{Z|X_0=x_0}$, and then
- (ii) sample Y from $\mathbb{P}_{Y|Z,X=x}$ by setting $\eta^* := h^*(Z, x, \xi)$ and applying $f^*(x, \eta^*)$.

According to (18), we know η^* follows the standard Gaussian for any x . Thus, we can simplify the above sampling procedure to directly sampling $\eta^* \sim \mathcal{N}(0, I_{d_y})$ and applying $f^*(x, \eta^*)$. This yields the last desired result that $f^*(x, \eta) \sim \mathbb{P}_{Y(x)}$. \square

A.3 Consistency of energy distance

If Assumptions 3.2 and 3.3 hold, we introduce the following Lemma:

Lemma A.1 (Concentration inequality with energy distance). *Let \mathbb{P} be a probability measure on $X \subseteq \mathbb{R}^d$, \mathbb{P}^n be the empirical measure obtained from n independently and identically distributed samples of \mathbb{P} , i.e. $\mathbb{P}^n = \frac{1}{n} \sum_{i=1}^n \delta_{x_i}$, $x_i \stackrel{\text{i.i.d.}}{\sim} \mathbb{P}$.*

For every $\delta > 0$, with probability at least $(1 - \delta)(1 - q_{R_n})$:

$$\text{ED}(\mathbb{P}, \mathbb{P}^n) < \frac{C_1 M}{\sqrt{n(1 - q_{R_n})}} + 4R_n \sqrt{\frac{2}{n} \log\left(\frac{1}{\delta}\right)},$$

for some constant $C_1 > 0$, where $R_n = \frac{3 \log n}{\alpha}$, $q_{R_n} := P(\max_{1 \leq i \leq n} \|x_i\| > R_n)$. We also have:

$$q_{R_n} \leq \frac{C}{n^2}.$$

We first prove the following lemma:

Lemma A.2 (Finite second moment of $\text{ED}(\mathbb{P}, \mathbb{P}^n)$). *For a probability measure \mathbb{P} that satisfies Assumption 3.2 and Assumption 3.3, where \mathbb{P}^n is the empirical distribution, there exists a constant $C_0 > 0$, such that $\mathbb{E}[\text{ED}(\mathbb{P}, \mathbb{P}^n)^2] \leq C_0 M^2/n$.*

Proof. We have

$$\text{ED}(\mathbb{P}, \mathbb{P}^n) = \frac{2}{n} \sum_{i=1}^n \mathbb{E}_{X \sim \mathbb{P}} \|X - x_i\| - \mathbb{E}_{X, X' \sim \mathbb{P}} \|X - X'\| - \frac{1}{n(n-1)} \sum_{j=1}^n \sum_{\substack{k=1 \\ k \neq j}}^n \|x_j - x_k\|.$$

We write $u(x) = \mathbb{E}_{X \sim \mathbb{P}} \|X - x\|$, $\nu = \mathbb{E}_{X, X' \sim \mathbb{P}} \|X - X'\|$, $U_n = \frac{1}{n(n-1)} \sum_{j=1}^n \sum_{\substack{k=1 \\ k \neq j}}^n \|x_j - x_k\|$. Clearly, $\mathbb{E}[U_n] = \nu$. We can thus write

$$\text{ED}(\mathbb{P}, \mathbb{P}^n) = \underbrace{\frac{2}{n} \sum_{i=1}^n (u(x_i) - \nu)}_{D_1} + \underbrace{(\nu - U_n)}_{D_2}.$$

For D_1 :

$$\text{Var}(D_1) = \frac{4}{n} \text{Var}(u(X) - \nu) = \frac{4}{n} \text{Var}(u(X)).$$

By Jensen's inequality, we have $u(x)^2 \leq \mathbb{E}_{X \sim \mathbb{P}} \|X - x\|^2$. Noting further that $\|X - x\|^2 \leq 2\|X\|^2 + 2\|x\|^2$, and applying Assumption 3.3, we get

$$\mathbb{E}_{X \sim \mathbb{P}} [u(X)^2] \leq 4M^2,$$

so that

$$\text{Var}(u(X) - \nu) = \mathbb{E}(u(X) - \nu)^2 \leq 4M^2$$

and

$$\text{Var}(D_1) \leq \frac{4 \cdot 4M^2}{n} = \frac{16M^2}{n}.$$

For D_2 , using the standard variance formula for U-statistics of order two (Hoeffding, 1948, equation 5.18), we obtain

$$\text{Var}(U_n) = \frac{4}{n} \sigma^2 + O\left(\frac{1}{n^2}\right),$$

where $\sigma^2 = \text{Var} [\mathbb{E}_{X, X' \sim \mathbb{P}} k(X, X')] = \text{Var}(u(X)) \leq 4M^2$. Thus,

$$\text{Var}(D_2) = \text{Var}(U_n) \leq \frac{16M^2}{n} + O\left(\frac{1}{n^2}\right),$$

which can be expressed as

$$\text{Var}(D_2) \leq \frac{C_2 M^2}{n},$$

for some constant $C_2 > 0$. We can therefore obtain

$$\mathbb{E}[\text{ED}(\mathbb{P}, \mathbb{P}^n)^2] \leq 2 \text{Var}(D_1) + 2 \text{Var}(D_2) + (\mathbb{E}D_2)^2$$

where $\mathbb{E}D_2 = 0$.

Thus we obtain

$$\mathbb{E}[\text{ED}(\mathbb{P}, \mathbb{P}^n)^2] \leq \frac{C_0 M^2}{n}$$

for some constant $C_0 > 0$. □

Proof of Lemma A.1. Let \mathcal{A}_{R_n} denote the event $\mathcal{A}_{R_n} := \{\max_{1 \leq i \leq n} \|X_i\| \leq R_n\}$. On \mathcal{A}_{R_n} , for any points $x, x' \sim \mathbb{P}$,

$$\|x - x'\| \leq \|x\| + \|x'\| \leq 2R_n.$$

With Assumption 3.2, we have

$$\begin{aligned} q_{R_n} &= P(\mathcal{A}_{R_n}^c) = P(\exists i, \|X_i\| > R_n) \leq nC \exp(-\alpha R_n) \\ &= nC \exp\left(-\alpha \frac{3 \log n}{\alpha}\right) \\ &= C/n^2. \end{aligned}$$

We can now follow a similar proof to that of Lemma 1 in Briol et al. (2019). Denote $h(x_1, \dots, x_n) = \text{ED}(\mathbb{P}, \mathbb{P}^n)$, explicitly we have

$$h(x_1, \dots, x_n) = \frac{2}{n} \sum_{i=1}^n \mathbb{E}_{X \sim \mathbb{P}} \|X - x_i\| - \mathbb{E}_{X, X' \sim \mathbb{P}} \|X - X'\| - \frac{1}{n(n-1)} \sum_{j=1}^n \sum_{\substack{k=1 \\ k \neq j}}^n \|x_j - x_k\|.$$

Only the first and last term can be affected by changing a single point from x_i to x'_i . On the event \mathcal{A}_R , the first term changes by at most

$$\begin{aligned} \frac{2}{n} \left| \mathbb{E} \|X - x_i\| - \mathbb{E} \|X - x'_i\| \right| &\leq \frac{2}{n} \mathbb{E} \left| \|X - x_i\| - \|X - x'_i\| \right| \\ &\leq \frac{2}{n} \|x_i - x'_i\| \\ &\leq \frac{2}{n} (\|x_i\| + \|x'_i\|). \end{aligned}$$

The first inequality follows from Jensen's inequality. On the event \mathcal{A}_{R_n} , we have

$$\frac{2}{n} \left| \mathbb{E} \|X - x_i\| - \mathbb{E} \|X - x'_i\| \right| \leq \frac{2}{n} (\|x_i\| + \|x'_i\|) \leq \frac{2}{n} \cdot 2R_n = \frac{4R_n}{n}.$$

For the last term $\frac{1}{n(n-1)} \sum_{j,k=1; j \neq k}^n \|x_j - x_k\|$, changing one sample point from x_i to x'_i resulting in changing $2n - 1$ pairs (pairs of form (x_i, x_j) for all $j = 1, \dots, n$ and pairs of form (x_j, x_i) for all $j \neq i$). Each pair changes by at most $\|x_i - x_j\| \leq 2R_n$. Thus, this term is bounded by $\frac{1}{n^2} (2n - 1) \cdot 2R_n \leq \frac{4R_n}{n}$.

Thus, on \mathcal{A}_R , for all $x_i, x'_i \in \mathcal{X}$, $i = 1, \dots, n$, we have

$$|h(x_1, x_2, \dots, x_i, \dots, x_n) - h(x_1, x_2, \dots, x'_i, \dots, x_n)| \leq \frac{4R_n}{n} + \frac{4R_n}{n} = \frac{8R_n}{n}.$$

By McDiarmid's inequality (McDiarmid, 1989), we get that for any $\epsilon > 0$,

$$\begin{aligned} P\left(\text{ED}(\mathbb{P}, \mathbb{P}^n) - \mathbb{E}[\text{ED}(\mathbb{P}, \mathbb{P}^n) \mid \mathcal{A}_{R_n}] \geq \epsilon \mid \mathcal{A}_{R_n}\right) &\leq \exp\left(-2\epsilon^2/\{n(8R_n/n)^2\}\right) \\ &= \exp\left(\frac{-n\epsilon^2}{32R_n^2}\right). \end{aligned}$$

By setting the probability to δ , we have $\epsilon = 4R_n \sqrt{\frac{2}{n} \log(\frac{1}{\delta})}$. Thus, we get that on the event \mathcal{A}_{R_n}

$$P\left(\text{ED}(\mathbb{P}, \mathbb{P}^n) - \mathbb{E}[\text{ED}(\mathbb{P}, \mathbb{P}^n) \mid \mathcal{A}_{R_n}] < 4R_n \sqrt{\frac{2}{n} \log\left(\frac{1}{\delta}\right)}\right) \geq 1 - \delta.$$

Observe that

$$\begin{aligned} \mathbb{E}[\text{ED}(\mathbb{P}, \mathbb{P}^n) \mid \mathcal{A}_{R_n}] &= \frac{\mathbb{E}[\text{ED}(\mathbb{P}, \mathbb{P}^n) \mathbb{1}(\mathcal{A}_{R_n})]}{P(\mathcal{A}_{R_n})} \\ &\leq \frac{\sqrt{\mathbb{E}[\text{ED}(\mathbb{P}, \mathbb{P}^n)]^2} \sqrt{P(\mathcal{A}_{R_n})}}{P(\mathcal{A}_{R_n})} \\ &\leq \frac{\sqrt{\mathbb{E}[\text{ED}(\mathbb{P}, \mathbb{P}^n)]^2}}{\sqrt{1 - q_{R_n}}} \\ &\leq \frac{C_1 M}{\sqrt{n(1 - q_{R_n})}}; \end{aligned}$$

here the last inequality is from Lemma A.2.

We thus obtain that conditioning on event \mathcal{A}_{R_n} :

$$P\left(\text{ED}(\mathbb{P}, \mathbb{P}^n) < \frac{C_1 M}{\sqrt{n(1-q_{R_n})}} + 4R_n \sqrt{\frac{2}{n} \log\left(\frac{1}{\delta}\right)}\right) \geq 1 - \delta,$$

and thus the unconditional probability is

$$P\left(\text{ED}(\mathbb{P}, \mathbb{P}^n) < \frac{C_1 M}{\sqrt{n(1-q_{R_n})}} + 4R_n \sqrt{\frac{2}{n} \log\left(\frac{1}{\delta}\right)}\right) \geq (1-\delta)P(\mathcal{A}_{R_n}) = (1-\delta)(1-q_{R_n}).$$

Combining all the above inequalities, we have with probability at least $(1-\delta)(1-q_{R_n})$:

$$\text{ED}(\mathbb{P}, \mathbb{P}^n) < \frac{C_1 M}{\sqrt{n(1-q_{R_n})}} + 4R_n \sqrt{\frac{2}{n} \log\left(\frac{1}{\delta}\right)},$$

with $q_{R_n} \leq C/n^2$. □

Theorem A.1 (Generalization bounds). *We write*

$$\hat{\theta}_n = \operatorname{argmin}_{\theta \in \Theta} \text{ED}(\mathbb{P}_\theta, \mathbb{Q}^n),$$

$$\hat{\theta}_{m,n} = \operatorname{argmin}_{\theta \in \Theta} \text{ED}(\mathbb{P}_\theta^m, \mathbb{Q}^n).$$

Assuming that for $X \sim \mathbb{Q}$, conditions in Lemma A.1 are satisfied, we have:

$$\text{ED}(\mathbb{P}_{\hat{\theta}_n}, \mathbb{Q}) - \inf_{\theta \in \Theta} \text{ED}(\mathbb{P}_\theta, \mathbb{Q}) < \frac{2C_1 M}{\sqrt{n(1-q_{R_n})}} + 8R_n \sqrt{\frac{2}{n} \log\left(\frac{1}{\delta}\right)}$$

with probability at least $(1-\delta)(1-q_{R_n})$.

If additionally we assume that for $Y \sim \mathbb{P}$, assumptions in Lemma A.1 are also satisfied, and denote $t = \max\{m, n\}$,

$$\mathcal{A}_{R_t} := \left\{ \max_{1 \leq i \leq n} \|x_i\| \leq R_t, \max_{1 \leq j \leq m} \|y_j\| \leq R_t \right\}$$

with $R_t = \frac{3 \log t}{\alpha}$. Then

$$\text{ED}(\mathbb{P}_{\hat{\theta}_{m,n}}, \mathbb{Q}) - \inf_{\theta \in \Theta} \text{ED}(\mathbb{P}_\theta, \mathbb{Q}) < \left(8R_t \sqrt{2 \log\left(\frac{1}{\delta}\right)} + \frac{2C_1 M}{\sqrt{1-q_{R_t}}} \right) \left(\frac{1}{\sqrt{n}} + \frac{1}{\sqrt{m}} \right)$$

with probability at least $(1-2\delta)(1-q_{R_t})$, where $q_{R_t} = P(\mathcal{A}_{R_t}^c)$ and $q_{R_t} \leq \frac{2C}{t^2}$.

Proof. Following the same notations in Lemma A.1, we that on events \mathcal{A}_{R_n} :

$$\begin{aligned} \text{ED}(\mathbb{P}_{\hat{\theta}_n}, \mathbb{Q}) - \inf_{\theta \in \Theta} \text{ED}(\mathbb{P}_\theta, \mathbb{Q}) &= \text{ED}(\mathbb{P}_{\hat{\theta}_n}, \mathbb{Q}) - \text{ED}(\mathbb{P}_{\hat{\theta}_n}, \mathbb{Q}^n) \\ &\quad + \text{ED}(\mathbb{P}_{\hat{\theta}_n}, \mathbb{Q}^n) - \inf_{\theta \in \Theta} \text{ED}(\mathbb{P}_\theta, \mathbb{Q}^n) \\ &\quad + \inf_{\theta \in \Theta} \text{ED}(\mathbb{P}_\theta, \mathbb{Q}^n) - \inf_{\theta \in \Theta} \text{ED}(\mathbb{P}_\theta, \mathbb{Q}) \\ &= \text{ED}(\mathbb{Q}, \mathbb{Q}^n) + \inf_{\theta \in \Theta} \text{ED}(\mathbb{P}_\theta, \mathbb{Q}^n) - \inf_{\theta \in \Theta} \text{ED}(\mathbb{P}_\theta, \mathbb{Q}) \\ &\leq 2 \sup \text{ED}(\mathbb{Q}, \mathbb{Q}^n), \end{aligned}$$

provided that $\text{ED}(\mathbb{P}_{\hat{\theta}_n}, \mathbb{Q}^n) = \inf_{\theta \in \Theta} \text{ED}(\mathbb{P}_\theta, \mathbb{Q}^n)$ and $\inf_{x \in \mathcal{X}} f(x) - \inf_{x \in \mathcal{X}} g(x) \leq \sup_{x \in \mathcal{X}} (f(x) - g(x))$, if $f(x), g(x)$ are bounded. As we condition on events \mathcal{A}_{R_n} , $\text{ED}(\mathbb{P}_\theta, \mathbb{Q})$, $\text{ED}(\mathbb{P}_\theta, \mathbb{Q}^n)$ are bounded.

Thus by Lemma A.1, we have

$$\text{ED}(\mathbb{P}_{\hat{\theta}_n}, \mathbb{Q}) - \inf_{\theta \in \Theta} \text{ED}(\mathbb{P}_\theta, \mathbb{Q}) < \frac{2C_1 M}{\sqrt{n(1 - q_{R_n})}} + 8R_n \sqrt{\frac{2}{n} \log\left(\frac{1}{\delta}\right)}$$

with probability at least $1 - \delta$ on the event \mathcal{A}_{R_n} . Following the same method, we know that with probability $(1 - \delta)(1 - q_{R_n})$, the above inequality stands without conditioning on event \mathcal{A}_{R_n} .

For $\text{ED}(\mathbb{P}_{\hat{\theta}_{m,n}}, \mathbb{Q}) - \inf_{\theta \in \Theta} \text{ED}(\mathbb{P}_\theta, \mathbb{Q})$, it is obvious that

$$\begin{aligned} q_{R_t} &= P(\mathcal{A}_{R_t}^c) \leq P(\{\exists j, \|Y_j\| \geq R_t\}) + P(\{\exists i, \|X_i\| \geq R_t\}) \\ &\leq (m+n)C \exp(-\alpha R_t) \\ &\leq 2tC \exp(-\alpha R_t) \\ &\leq \frac{2C}{t^2}. \end{aligned}$$

We decompose $\text{ED}(\mathbb{P}_{\hat{\theta}_{m,n}}, \mathbb{Q}) - \inf_{\theta \in \Theta} \text{ED}(\mathbb{P}_\theta, \mathbb{Q})$ as

$$\begin{aligned} \text{ED}(\mathbb{P}_{\hat{\theta}_{m,n}}, \mathbb{Q}) - \inf_{\theta \in \Theta} \text{ED}(\mathbb{P}_\theta, \mathbb{Q}) &= \text{ED}(\mathbb{P}_{\hat{\theta}_{m,n}}, \mathbb{Q}) - \text{ED}(\mathbb{P}_{\hat{\theta}_{m,n}}^m, \mathbb{Q}) \\ &\quad + \text{ED}(\mathbb{P}_{\hat{\theta}_{m,n}}^m, \mathbb{Q}) - \text{ED}(\mathbb{P}_{\hat{\theta}_{m,n}}^m, \mathbb{Q}^n) \\ &\quad + \text{ED}(\mathbb{P}_{\hat{\theta}_{m,n}}^m, \mathbb{Q}^n) - \inf_{\theta \in \Theta} \text{ED}(\mathbb{P}_\theta^m, \mathbb{Q}) \\ &\quad + \inf_{\theta \in \Theta} \text{ED}(\mathbb{P}_\theta^m, \mathbb{Q}) - \inf_{\theta \in \Theta} \text{ED}(\mathbb{P}_\theta, \mathbb{Q}). \end{aligned}$$

On the event \mathcal{A}_{R_t} , note that

$$\text{ED}(\mathbb{P}_{\hat{\theta}_{m,n}}, \mathbb{Q}) - \text{ED}(\mathbb{P}_{\hat{\theta}_{m,n}}^m, \mathbb{Q}) = \text{ED}(\mathbb{P}_{\hat{\theta}_{m,n}}, \mathbb{P}_{\hat{\theta}_{m,n}}^m) \leq \sup_{\theta \in \Theta} \text{ED}(\mathbb{P}_\theta, \mathbb{P}_\theta^m),$$

$$\text{ED}(\mathbb{P}_{\hat{\theta}_{m,n}}^m, \mathbb{Q}) - \text{ED}(\mathbb{P}_{\hat{\theta}_{m,n}}^m, \mathbb{Q}^n) = \text{ED}(\mathbb{Q}, \mathbb{Q}^n),$$

$$\text{ED}(\mathbb{P}_{\hat{\theta}_{m,n}}^m, \mathbb{Q}^n) - \inf_{\theta \in \Theta} \text{ED}(\mathbb{P}_\theta^m, \mathbb{Q}) = \inf_{\theta \in \Theta} \text{ED}(\mathbb{P}_\theta^m, \mathbb{Q}^n) - \inf_{\theta \in \Theta} \text{ED}(\mathbb{P}_\theta^m, \mathbb{Q}) \leq \sup \text{ED}(\mathbb{Q}, \mathbb{Q}^n),$$

and

$$\inf_{\theta \in \Theta} \text{ED}(\mathbb{P}_\theta^m, \mathbb{Q}) - \inf_{\theta \in \Theta} \text{ED}(\mathbb{P}_\theta, \mathbb{Q}) \leq \sup_{\theta \in \Theta} \text{ED}(\mathbb{P}_\theta, \mathbb{P}_\theta^m).$$

As derived in Lemma A.1, on the event \mathcal{A}_{R_t} we have

$$\begin{aligned} P\left(\text{ED}(\mathbb{P}_\theta, \mathbb{P}_\theta^m) \geq 4R_t \sqrt{\frac{2}{m} \log\left(\frac{1}{\delta}\right)} + \frac{C_1 M}{\sqrt{m(1 - q_{R_t})}}\right) &< \delta \\ P\left(\text{ED}(\mathbb{Q}, \mathbb{Q}^n) \geq 4R_t \sqrt{\frac{2}{n} \log\left(\frac{1}{\delta}\right)} + \frac{C_1 M}{\sqrt{n(1 - q_{R_t})}}\right) &< \delta. \end{aligned}$$

Thus

$$P\left(\left(2\sup_{\theta \in \Theta} \text{ED}(\mathbb{P}_\theta, \mathbb{P}_\theta^m) + 2\sup \text{ED}(\mathbb{Q}, \mathbb{Q}^n)\right) < \left(8R_t \sqrt{2 \log\left(\frac{1}{\delta}\right)} + \frac{2C_1 M}{\sqrt{1-q_{R_t}}}\right) \left(\frac{1}{\sqrt{n}} + \frac{1}{\sqrt{m}}\right)\right) \geq 1 - 2\delta$$

conditioning on the event \mathcal{A}_{R_t} .

Combining all these together, we obtain that unconditionally

$$\begin{aligned} \text{ED}(\mathbb{P}_{\hat{\theta}_{m,n}}, \mathbb{Q}) - \inf_{\theta \in \Theta} \text{ED}(\mathbb{P}_\theta, \mathbb{Q}) &\leq 2\sup_{\theta \in \Theta} \text{ED}(\mathbb{P}_\theta, \mathbb{P}_\theta^m) + 2\sup \text{ED}(\mathbb{Q}, \mathbb{Q}^n) \\ &< \left(8R_t \sqrt{2 \log\left(\frac{1}{\delta}\right)} + \frac{2C_1 M}{\sqrt{1-q_{R_t}}}\right) \left(\frac{1}{\sqrt{n}} + \frac{1}{\sqrt{m}}\right) \end{aligned}$$

with probability at least $(1 - 2\delta)(1 - q_{R_t})$. \square

With the above theorems, we can now prove Theorem 3.1.

Proof of Theorem 3.1. This proof is similar to that of Proposition 1 in Briol et al. (2019).

Given $n \in \mathbb{N}$, define the event

$$\mathcal{A}_n = \left\{ \left| \text{ED}(\mathbb{P}_{\hat{\theta}_n}, \mathbb{Q}) - \inf_{\theta \in \Theta} \text{ED}(\mathbb{P}_\theta, \mathbb{Q}) \right| \geq 8R_n \sqrt{\frac{\log n}{n}} + \frac{2C_1 M}{\sqrt{n(1-q_{R_n})}} \right\}.$$

From Theorem A.1 we know that $\mathbb{Q}(\mathcal{A}_n) \leq 1 - (1 - \delta)(1 - q_{R_n}) \leq 1 - (1 - \delta) \leq \delta = 1/n^2$ (as we set $\delta = 1/n^2$ and $q_{R_n} \leq C/n^2$). Thus, $\sum_n \mathbb{Q}(\mathcal{A}_n) < \infty$. Using the Borel-Cantelli lemma, we know that \mathbb{Q} -almost surely, there exists $N > 0$ such that for all $n \geq N$,

$$\text{ED}(\mathbb{P}_{\hat{\theta}_n}, \mathbb{Q}) - \inf_{\theta \in \Theta} \text{ED}(\mathbb{P}_\theta, \mathbb{Q}) < 8R_n \sqrt{\frac{\log n}{n}} + \frac{2C_1 M}{\sqrt{n(1-q_{R_n})}}.$$

We have convergence results of the RHS:

$$8R_n \sqrt{\frac{\log n}{n}} = \Theta\left(\frac{(\log n)^{\frac{3}{2}}}{\sqrt{n}}\right)$$

and $(\log n)^{\frac{3}{2}}/\sqrt{n} \rightarrow 0$.

We also obtain

$$\frac{2C_1 M}{\sqrt{n(1-q_{R_n})}} = O\left(\frac{C_3}{n}\right)$$

which converges to 0 as $n \rightarrow \infty$, since $1 - q_{R_n} \rightarrow 1$. The consistency of $\hat{\theta}_{m,n}$ can be proved similarly. \square

A.4 Proof of Proposition 4.1

Proof. Since $\tilde{\eta}$ is a continuous random variable, there exists a strictly monotone function \tilde{f}_1 such that $\tilde{\eta} \stackrel{d}{=} \tilde{f}_1(\tilde{\xi})$ where $\tilde{\xi} \sim \mathcal{N}(0, 1)$. Let f^*, f_1^* denotes the element of an optimal fregression model such that

$$f^*(x + f_1^*(\tilde{\xi})) \sim \mathbb{P}_{Y(x)},$$

for all $x \in \mathcal{X}$ by Proposition 2.2. This implies

$$\tilde{f}(x + \tilde{f}_1(\tilde{\xi})) \stackrel{d}{=} f^*(x + f_1^*(\tilde{\xi})),$$

for all $x \in \mathcal{X}$. Since $\tilde{f}, \tilde{f}_1, f^*$, and f_1^* are strictly monotone, we assume without loss of generality that all of them are strictly increasing.

For any $\tilde{\alpha} \in [0, 1]$, by taking the $\tilde{\alpha}$ -quantile on both sides and letting α denote the $\tilde{\alpha}$ -quantile of the standard Gaussian distribution, we have

$$\tilde{f}(x + \tilde{f}_1(\alpha)) = f^*(x + f_1^*(\alpha)), \quad (19)$$

for all $x \in \mathcal{X}$ and $\alpha \in \mathbb{R}$. Taking the derivative w.r.t. x and α respectively yields

$$\begin{aligned} \tilde{f}'(x + \tilde{f}_1(\alpha)) &= f_1'^*(x + f_1^*(\alpha)) \\ \tilde{f}'(x + \tilde{f}_1(\alpha))\tilde{f}_1'(\alpha) &= f_1'^*(x + f_1^*(\alpha))f_1^{*\prime}(\alpha). \end{aligned}$$

Taking the ratio of these two equations leads to $\tilde{f}_1'(\alpha) = f_1'^*(\alpha)$, which implies $\tilde{f}(\alpha) = f_1^*(\alpha) + c$ for some constant c , for all $\alpha \in \mathbb{R}$. Assume without loss of generality that $f_1^*(0) = 0$ and we know from the fact that $\tilde{\eta}$ has a median 0; thus $c = 0$, that is, $\tilde{f}_1(\alpha) = f_1^*(\alpha)$ for all $\alpha \in \mathbb{R}$.

Then according to (19), we have

$$\tilde{f}(\tilde{x}) = f^*(\tilde{x}),$$

for all $\tilde{x} \in [x_{\min} - \tilde{\eta}_0, x_{\max} + \tilde{\eta}_0]$. Note that $\tilde{f}(x)$ and $f^*(x)$ are exactly the true and modelled conditional medians, respectively; the desired result then follows. \square

B Hyperparameters in fregression

All hyperparameters are kept the same in the experiments in the paper except for number of epochs, which is chosen so that the loss converges. The hyperparameters include

- `learning_rate`: The learning rate is set to be 10^{-4} .
- `hidden_layer`: The number of hidden layers in the neural network is set to be 3.
- `hidden_dim`: The size of neurons per hidden layer is set to be 100.

C Experiment details

All experiments were conducted on MacBook with an Apple M3 chip, 8-core CPU, and 32GB RAM.

C.1 Binary intervention

In this setting, for each simulation, we train fregression for 1000 epochs.

For the AIPW estimator, we fit the propensity score model with logistic regression; because the true propensity scores are linear in the covariates, this specification performs well. We model the outcomes separately using random forests.

Next, we compare fregression to two advanced deep neural network approaches for causal inference, CausalEGM and Dragonnet. A comprehensive list of CausalEGM’s hyper-parameters is available at https://causalegm.readthedocs.io/en/latest/tutorial_py.html. Because the search space is extensive, we adopt the configuration recommended for the binary treatment experiments in the original paper. The settings of key hyperparameters are given in Table 4; all other quantities remain at their default values. Although the authors of CausalEGM suggest 30,000 epochs especially for continuous treatment setting, for fair comparison we train CausalEGM for 1000 epochs in our experiments.

Hyperparameter	Value
Latent covariate dimensions: z_dims	[1, 1, 1, 1]
Learning rate: lr	2×10^{-4}
Reconstruction loss weight: alpha	1
Round trip loss weight: beta	1
Gradient penalty loss weight: gamma	10
Generator units: g_units	[64, 64, 64, 64, 64]
Encoder units: e_units	[64, 64, 64, 64, 64]
F network units: f_units	[64, 32, 8]
H network units: h_units	[64, 32, 8]
Discriminator units in latent space: dz_units	[64, 32, 8]
Discriminator units in covariate space: dv_units	[64, 32, 8]

Table 4: Values of key hyperparameters in the CausalEGM model.

For Dragonnet, in line its requirements, we tuned the hyperparameters with `optuna`. The search range is shown in Table 5. We conduct 30 hyperparameter searching trials, selecting the best configuration by validation performance on a hold out set of 400 samples, and then apply the resulting model to an independent test set of 400 samples to obtain the reported estimates.

C.2 Longitudinal Analysis

C.2.1 Synthetic Data

We provide the details of the synthetic data generation in Section 6.3.

Hyperparameter	Value
Learning rate: lr	logUniform($10^{-5}, 10^{-2}$)
Weights decay rate: wd	logUniform($10^{-5}, 10^{-2}$)
Batch size: bs	{32, 128, 256}
Number of iterations: epochs	Grid search in between 200 and 600
Number of neurons in shared layers: shared_hidden	Grid search in between 50 and 200
Number of neurons in shared layers: outcome_hidden	Grid search in between 50 and 200

Table 5: Search ranges of key hyperparameters in the Dragonnet model.

	Setting 1	Setting 2	Setting 3
C	Bernoulli(0.5)	Exp(1)	Bernoulli(0.5)
$Z_t \mid \bar{X}_{t-1}, C$	$\mathcal{N}(-0.5 + 0.5X_{t-1} + 0.25C, 0.5)$	$\mathcal{N}(0.7Z_{t-1} + 0.2X_{t-1})$	$\mathcal{N}(-0.5 + 0.5X_{t-1} + 0.25C, 0.5)$
$X_t \mid \bar{Z}_t, C$	Bernoulli($0.2Z_t + 0.1$)	Bernoulli($-0.5 + 0.25X_{t-1} + 0.5Z_t$)	$\mathcal{N}(1.2 + 0.1Z_t + 2C, 0.1)$
$\tilde{Y}_t(\bar{x}_t) \mid C$	Exp($0.3 + 0.2x_t + 0.1C$)	Exp($0.5 + 0.2x_t + 0.2C, 1$)	Exp($0.1 + 0.3x_t + 0.1C$)
Gaussian copula (with Pearson correlation ρ)	$\rho = 0.4$ between Z_t and Y_t	pair-copula: $\rho_{Y_t, Z_{t-1}} = 0.2$, $\rho_{Y_t, Z_t \mid Z_{t-1}} = 0.3$ (depends on C)	$\rho = 0.4$ between Z_t and Y_t

Table 6: Simulation settings 1–3.

C.2.2 Survival Analysis: comparison with `dltmle`

In our implementation of `dltmle` (Shirakawa, 2024) in Section 6.3, we tuned the hyperparameters using their built in `dltmle.tune` function within the candidates in Table 8.

C.3 LEADER

We provide the description of each variable name in our experiment on the LEADER trial in Table 9.

References

Abadie, A. (2002). Bootstrap tests for distributional treatment effects in instrumental variable models. *Journal of the American Statistical Association* 97(457), 284–292.

Athey, S., G. W. Imbens, J. Metzger, and E. Munro (2024). Using Wasserstein generative adversarial networks for the design of Monte Carlo simulations. *Journal of Econometrics* 240(2), 105076.

Bitler, M. P., J. B. Gelbach, and H. W. Hoynes (2017). Can variation in subgroups’ average treatment effects explain treatment effect heterogeneity? Evidence from a social experiment. *Review of Economics and Statistics* 99(4), 683–697.

Setting 4	
C	$\mathcal{N}(0, 1)$
$Z_t \bar{X}_{t-1}, C$	$\mathcal{N}(-0.5 + 0.5X_{t-1} + 0.5Z_{t-1} + 0.5C, 0.5)$
$X_t \bar{Z}_t, C$	$\mathcal{N}(2Z_t + 0.1C, 1)$
$Y_t(\bar{x}_t) C$	$\mathcal{N}(2x_t + x_{t-1} + 0.5x_{t-2} + C, 1)$
Gaussian copula with Pearson correlation ρ	$\rho = 0.24$

Table 7: Simulation setting 4.

Hyperparameter	Hyperparameter values / candidates for search
dim_emb	{8, 16}
dim_emb_time	{4, 8}
dim_emb_type	{4, 8}
hidden_size	{8, 16, 32}
num_layers	{1, 2, 4}
nhead	{2, 4}
dropout	{0, 0.1, 0.2}
learning_rate	{ 10^{-3} , 5×10^{-4} , 10^{-4} , 5×10^{-3} }
alpha	[0.05, 0.1, 0.5, 1]
beta	[0.05, 0.1, 0.5, 1]

Table 8: Search ranges of key hyperparameters of `dltmle` model.

Briol, F.-X., A. Barp, A. B. Duncan, and M. Girolami (2019). Statistical inference for generative models with maximum mean discrepancy. *arXiv preprint arXiv:1906.05944*.

Chernozhukov, V., D. Chetverikov, M. Demirer, E. Duflo, C. Hansen, W. Newey, and J. Robins (2018, 01). Double/debiased machine learning for treatment and structural parameters. *The Econometrics Journal* 21(1), C1–C68.

de Vassimon Manela, D., L. Battaglia, and R. Evans (2024). Marginal causal flows for validation and inference. *Advances in Neural Information Processing Systems* 37, 9920–9949.

Díaz, I. (2017). Efficient estimation of quantiles in missing data models. *Journal of Statistical Planning and Inference* 190, 39–51.

Dwork, C., F. McSherry, K. Nissim, and A. Smith (2006). Calibrating noise to sensitivity in private data analysis. In *Theory of Cryptography: Third Theory of Cryptography Conference, TCC 2006, New York, NY, USA, March 4–7, 2006. Proceedings* 3, pp. 265–284. Springer.

Evans, R. J. (2021a). `causl`. <https://github.com/rje42/causl>.

Evans, R. J. (2021b). `survivl`. <https://github.com/rje42/survivl>.

Variable	Description
SEX.F	Binary variable. If <code>True</code> , the patient is female.
SMOKER_NEVER.Smoked.	Binary variable. If <code>True</code> , the patient has never smoked before.
STENFL	Carotid $> 50\%$ stenosis on angiography. Binary.
NEPSCRFL	Diabetic Nephropathy at screening flag. Binary.
Age	Patient's age when enrolled in the trial.
DIABDUR	Diabetes duration (years) at baseline.
HDL1BL	HDL Cholesterol (mmol/L) at baseline.
LDL1BL	LDL Cholesterol (mmol/L) at baseline.
CHOL1BL	Total Cholesterol (mmol/L) at baseline.
log_TRIG1BL	Logarithm of triglycerides (mmol/L) at baseline.
log_CREATBL	Serum Creatinine ($\mu\text{mol}/\text{L}$) at baseline.

Table 9: Description of each variable in used in Section 7.

Evans, R. J. and V. Didelez (2024). Parameterizing and simulating from causal models (with discussion). *Journal of the Royal Statistical Society Series B: Statistical Methodology* 86(3), 535–568.

Frauen, D., T. Hatt, V. Melnychuk, and S. Feuerriegel (2023). Estimating average causal effects from patient trajectories. In *Proceedings of the Thirty-Seventh AAAI Conference on Artificial Intelligence*, pp. 7586–7594.

Friedrich, S. and T. Friede (2024). On the role of benchmarking data sets and simulations in method comparison studies. *Biometrical Journal* 66(1), 2200212.

Gamella, J. L., J. Peters, and P. Bühlmann (2025). Causal chambers as a real-world physical testbed for AI methodology. *Nature Machine Intelligence*, 1–12.

Giuffrè, M. and D. L. Shung (2023). Harnessing the power of synthetic data in healthcare: innovation, application, and privacy. *NPJ digital medicine* 6(1), 186.

Gneiting, T. and A. E. Raftery (2007). Strictly proper scoring rules, prediction, and estimation. *Journal of the American Statistical Association* 102(477), 359–378.

Hahn, P. R., J. S. Murray, and C. M. Carvalho (2020). Bayesian regression tree models for causal inference: Regularization, confounding, and heterogeneous effects (with discussion). *Bayesian Analysis* 15(3), 965–1056.

Havercroft, W. and V. Didelez (2012). Simulating from marginal structural models with time-dependent confounding. *Statistics in Medicine* 31(30), 4190–4206.

Hernán, M. A. and J. M. Robins (2025). *Causal Inference: What If*. Boca Raton: Chapman & Hall/CRC.

Hirano, K. and G. W. Imbens (2004). *The Propensity Score with Continuous Treatments*, Chapter 7, pp. 73–84. John Wiley & Sons, Ltd.

Hoeffding, W. (1948). A class of statistics with asymptotically normal distribution. *The Annals of Mathematical Statistics* 19(3), 293–325.

Holovchak, A., S. Saengkyongam, N. Meinshausen, and X. Shen (2025). Distributional instrumental variable method. *arXiv preprint arXiv:2502.07641*.

Huang, C.-W., D. Krueger, A. Lacoste, and A. Courville (2018). Neural autoregressive flows. In *International Conference on Machine Learning*, pp. 2078–2087. PMLR.

Kamthe, S., S. Assefa, and M. Deisenroth (2021). Copula flows for synthetic data generation. *arXiv preprint arXiv:2101.00598*.

Kennedy, E. H., S. Balakrishnan, and L. Wasserman (2023). Semiparametric counterfactual density estimation. *Biometrika* 110(4), 875–896.

Kenny, C. T., S. Kuriwaki, C. McCartan, E. T. Rosenman, T. Simko, and K. Imai (2021). The use of differential privacy for census data and its impact on redistricting: The case of the 2020 US Census. *Science Advances* 7(41), eabk3283.

Lendle, S. D., J. Schwab, M. L. Petersen, and M. J. van der Laan (2017). ltmle: an R package implementing targeted minimum loss-based estimation for longitudinal data. *Journal of Statistical Software* 81, 1–21.

Lin, X., D. d. V. Manela, C. Mathis, J. M. Tarp, and R. J. Evans (2025). Simulating longitudinal data from marginal structural models. *arXiv preprint arXiv:2502.07991*.

Liu, Q., Z. Chen, and W. H. Wong (2024). An encoding generative modeling approach to dimension reduction and covariate adjustment in causal inference with observational studies. *Proceedings of the National Academy of Sciences* 121(23), e2322376121.

Liu, Q. and W. H. Wong (2025). An AI-powered Bayesian generative modeling approach for causal inference in observational studies. *arXiv preprint arXiv:2501.00755*.

Louizos, C., U. Shalit, J. M. Mooij, D. Sontag, R. Zemel, and M. Welling (2017). Causal effect inference with deep latent-variable models. *Advances in Neural Information Processing Systems* 30.

Marso, S. P., G. H. Daniels, K. Brown-Frandsen, P. Kristensen, J. F. Mann, M. A. Nauck, S. E. Nissen, S. Pocock, N. R. Poulter, L. S. Ravn, et al. (2016). Liraglutide and cardiovascular outcomes in type 2 diabetes. *New England Journal of Medicine* 375(4), 311–322.

McCartan, C., T. Simko, and K. Imai (2023). Making differential privacy work for census data users. *Harvard Data Science Review* 10.

McDiarmid, C. (1989). On the method of bounded differences. *Surveys in Combinatorics* 141(1), 148–188.

Muandet, K., K. Fukumizu, B. Sriperumbudur, B. Schölkopf, et al. (2017). Kernel mean embedding of distributions: A review and beyond. *Foundations and Trends in Machine Learning* 10(1-2), 1–141.

Neal, B., C.-W. Huang, and S. Raghupathi (2020). RealCause: Realistic causal inference benchmarking. *arXiv preprint arXiv:2011.15007*.

Neyman, J. (1923). Sur les applications de la theorie des probabilités aux expériences agricoles: Essai des principes. Excerpts reprinted (1990) in English. *Statistical Science* 5(463-472), 4.

Novo Nordisk A/S (2015). Liraglutide effect and action in diabetes: Evaluation of cardiovascular outcome results (leader). <https://clinicaltrials.gov/study/NCT01179048>. NLM Identifier: NCT01179048.

Parikh, H., C. Varjao, L. Xu, and E. T. Tchetgen (2022). Validating causal inference methods. In *International Conference on Machine Learning*, pp. 17346–17358. PMLR.

Park, J., U. Shalit, B. Schölkopf, and K. Muandet (2021). Conditional distributional treatment effect with kernel conditional mean embeddings and U-statistic regression. In *International Conference on Machine Learning*, pp. 8401–8412. PMLR.

Pearl, J. (2009). *Causality*. Cambridge University Press.

Pezoulas, V. C., D. I. Zaridis, E. Mylona, C. Androultsos, K. Apostolidis, N. S. Tachos, and D. I. Fotiadis (2024). Synthetic data generation methods in healthcare: A review on open-source tools and methods. *Computational and Structural Biotechnology Journal*.

Richardson, T. S. and J. M. Robins (2013). Single world intervention graphs (SWIGs): A unification of the counterfactual and graphical approaches to causality. *Center for the Statistics and the Social Sciences, University of Washington Series. Working Paper* 128(30), 2013.

Rubin, D. B. (1974). Estimating causal effects of treatments in randomized and nonrandomized studies. *Journal of Educational Psychology* 66(5), 688.

Sejdinovic, D., B. Sriperumbudur, A. Gretton, and K. Fukumizu (2013). Equivalence of distance-based and RKHS-based statistics in hypothesis testing. *Annals of Statistics* 41(5), 2263–2291.

Shalit, U., F. D. Johansson, and D. Sontag (2017). Estimating individual treatment effect: generalization bounds and algorithms. In *International Conference on Machine Learning*, pp. 3076–3085. PMLR.

Shen, X. and N. Meinshausen (2024). Engression: extrapolation through the lens of distributional regression. *Journal of the Royal Statistical Society Series B: Statistical Methodology*, qkae108.

Shi, C., D. Blei, and V. Veitch (2019). Adapting neural networks for the estimation of treatment effects. *Advances in Neural Information Processing Systems* 32.

Shirakawa, T. (2024). dltmle python package (2024). <https://github.com/shirakawatoru/dltmle>.

Shirakawa, T., Y. Li, Y. Wu, S. Qiu, Y. Li, M. Zhao, H. Iso, and M. Van Der Laan (2024). Longitudinal targeted minimum loss-based estimation with temporal-difference heterogeneous transformer. *arXiv preprint arXiv:2404.04399*.

Sun, W., P. Wang, D. Yin, J. Yang, and Y. Chang (2015). Causal inference via sparse additive models with application to online advertising. In *Proceedings of the AAAI Conference on Artificial Intelligence*, Volume 29.

Székely, G. J. and M. L. Rizzo (2013). Energy statistics: A class of statistics based on distances. *Journal of Statistical Planning and Inference* 143(8), 1249–1272.

van der Laan, M. J. and S. Gruber (2012). Targeted minimum loss based estimation of causal effects of multiple time point interventions. *The International Journal of Biostatistics* 8(1).

Venturini, S., F. Dominici, and G. Parmigiani (2015). Generalized quantile treatment effect: A flexible Bayesian approach using quantile ratio smoothing. *Bayesian Analysis* 10(3), 523–552.

Wager, S. and S. Athey (2018). Estimation and inference of heterogeneous treatment effects using random forests. *Journal of the American Statistical Association* 113(523), 1228–1242.

Xu, D., M. J. Daniels, and A. G. Winterstein (2018). A Bayesian nonparametric approach to causal inference on quantiles. *Biometrics* 74(3), 986–996.

Yoon, J., L. N. Drumright, and M. Van Der Schaar (2020). Anonymization through data synthesis using generative adversarial networks (ADS-GAN). *IEEE Journal of Biomedical and Health Informatics* 24(8), 2378–2388.